Finnish Institute of Occupational Health

Evaluation of the health effects of carbon nanotubes

FINAL REPORT ON PROJECT NUMBER 109137
OF THE FINNISH WORK ENVIRONMENT FUND

Elina Rydman
Julia Catalán
Penny Nymark
Jaana Palomäki
Hannu Norppa
Harri Alenius
Joonas Koivisto
Henrik Wolff
Kaarle Hämeri
Lea Pylkkänen
Hilkka Järventaus
Satu Suhonen
Kirsi Siivola
Timo Tuomi
Merja Järvelä
Esa Vanhala
Jenni Rantala
Minnamari Vippola
Kai Savolainen

Finnish Institute of Occupational Health

Evaluation of the health effects of carbon nanotubes

FINAL REPORT ON PROJECT NUMBER 109137 OF THE FINNISH WORK ENVIRONMENT FUND

Elina Rydman, Julia Catalán, Penny Nymark, Jaana Palomäki, Hannu Norppa, Harri Alenius, Joonas Koivisto, Henrik Wolff, Kaarle Hämeri, Lea Pylkkänen, Hilkka Järventaus, Satu Suhonen, Kirsi Siivola, Timo Tuomi, Merja Järvelä, Esa Vanhala, Jenni Rantala, Minnamari Vippola, Kai Savolainen

Finnish Institute of Occupational Health

Helsinki 2013

Finnish Institute of Occupational Health

Nanosafety Research Centre

Topeliuksenkatu 41 a A

00250 Helsinki

www.ttl.fi

Editors: Elina Rydman (née Rossi), Julia Catalán, Penny Nymark, Jaana Palomäki, Hannu Norppa

Photos: Minnamari Vippola (nanomaterials in Fig. 1), Esa Vanhala (asbestos in Fig. 1), Joonas Koivisto (Fig. 2, right panel in Fig. 3), Elina Rydman (left panel in Fig. 3, Figs 14 and 18), Jukka Sund (Fig. 4)

Cover: Albert Hall Finland Oy Ltd

This publication has been accomplished with the support of the Finnish Work Environment Fund (Project No. 109137; "Hiilinanoputkien terveysvaikutusten arviointi")

ISBN 978-952-261-319-6 (paperback)

ISBN 978-952-261-320-2 (PDF)

Juvenes Print, Tampere 2013

SUMMARY

Carbon nanotubes are among the most important nanomaterials and their production and industrial use are rapidly growing. Long and rigid carbon nanotubes have been described to have similar adverse effects as asbestos. The purpose of the present project was to assess how carbon nanotubes induce pulmonary inflammation and fibrosis and if these phenomena involve genotoxic alterations which may be important in the formation of malignant tumors. In addition, complementary studies were performed *in vitro* to further understand the cellular effects of carbon nanotubes. Mice were exposed to two types (needle-like and tangled) of long, multi-walled carbon nanotubes (MWCNTs) by pharyngeal aspiration (10-200 µg/mouse) and inhalation (8 mg/m³) for 4 h or 4 days (4 h/day). Immunotoxic and genotoxic effects in the lungs were studied by using e.g. different molecular biological, histological, and cytogenetic methods and electron and light microscopy. Cultured human macrophages –cells of first line immune defense – were exposed to various types of carbon nanomaterials and crocidolite asbestos, and immunotoxic effects were examined by e.g. assessing the expression of selected inflammatory cytokines and chemokines and by inhibiting some of them. Human bronchial epithelial cells were exposed *in vitro* to MWCNTs, and cytotoxic and genotoxic effects were assessed by fluorescence microscopy. Long, needle-like MWCNTs caused inflammation in mice and in cultured macrophages. In the lungs, the effect was seen as a clear increase of inflammatory cells, certain cytokines and chemokines; the inflammatory reaction was stronger than seen with crocidolite asbestos. IL-1β and the inflammasome complex appeared to play a central role in the inflammatory process. The type and extent of the inflammatory effect depended on the route of exposure. Needle-like MWCNTs induced a much clearer inflammation when given by inhalation than by pharyngeal aspiration. The inflammation caused by inhaled MWCNTs greatly resembled allergic asthma, which is an unusual finding. Needle-like MWCTs also increased DNA damage in lung cells both after pharyngeal aspiration and inhalation exposure. In the inhalation experiments, a clear genotoxic effect was seen in broncho-alveolar lavage cells consisting mostly of macrophages**.** The genotoxic effect of MWCNTs was local – no alterations were seen in blood cells. Long, needle-like MWCNTs caused DNA damage also in cultures of bronchial epithelial cells. Long, tangled MWCNTs were not genotoxic in mice and induced only a marginal increase in DNA damage *in vitro*. Our studies agree with the idea that long, needle-like MWCNTs are hazardous, showing effects that have not previously been described such as asthma-like inflammation and DNA damage in the lungs. The rigidity of long, needle-like MWCNTs is probably a central characteristic determining their health effects. Rigid, needle-like MWCNTs with a diameter of >50 nm caused a strong inflammation and were genotoxic, while thinner (diameter ~ 8-15 nm), tangled MWCNTs did not have similar effects. It appears that long, needle-like MWCNTs should be handled with special caution.

TIIVISTELMÄ

Hiilinanoputket ovat tärkeimpiä nanomateriaaleja, ja niiden tuotanto ja teknologinen käyttö on kasvanut nopeasti. Pitkillä ja jäykillä hiilinanoputkikuiduilla on havaittu samoja haittavaikutuksia kuin asbestilla. Tämän hankkeen tavoitteena oli selvittää, miten hiilinanoputkien aiheuttama keuhkokudoksen tulehdus ja soluvälifibroosi syntyvät ja liittyykö näihin ilmiöihin genotoksisia muutoksia, joilla katsotaan olevan merkitystä pahanlaatuisten kasvainten synnyssä. Eläinkokeista saatuja tuloksia täydennettiin ja selvennettiin soluviljelmissä tehdyillä tutkimuksilla. Hiiriä altistettiin kahden tyyppisille (neulamaisille ja taipuisille), pitkille, moniseinäisille hiilinanoputkille ja krokidoliitti-asbestille aspiraatio-tekniikalla (10-200 µg/hiiri) sekä hengitysteitse (8 mg/m³) 4 tunnin tai 4 päivän (4 h/päivä) ajan. Immunotoksisia ja genotoksisia vaikutuksia keuhkoissa tutkittiin mm. käyttäen erilaisia molekyylibiologisia, histologisia, ja sytogeneettisiä menetelmiä sekä elektroni- ja valomikroskopiaa. Soluviljelmissä ihmisen makrofageja, etulinjan immuunipuolustussoluja, altistettiin erilaisille hiilinanomateriaaleille ja krokidoliitti-asbestille, ja immunotoksisia vaikutuksia tutkittiin mm. selvittämällä tulehdusta kuvaavien välittäjäaineiden ilmentymistä ja estämällä eräitä niistä. Ihmisen viljeltyjä keuhkoepiteelisoluja altistettiin hiilinanoputkille, ja solutoksisia sekä genotoksisia vaikutuksia tutkittiin fluoresenssimikroskoopilla. Pitkät, neulamaiset hiilinanoputket aiheuttivat tulehdusta sekä hiirissä että soluviljelmissä. Keuhkoissa vaikutus näkyi tulehdussolujen ja tulehdusta ilmentävien välittäjäaineiden selkeänä lisääntymisenä, ja tulehdusreaktio oli voimakkaampi kuin krokidoliitti-asbestilla. Välittäjäaine IL-1β ja inflammasomi-kompleksi näyttivät olevan tulehdusmekanismissa keskeisessä asemassa. Tulehdusreaktion laatu ja voimakkuus riippuivat altistustavasta. Neulamaiset hiilinanoputket aiheuttivat huomattavasti vakavamman tulehduksen hengitysilman kautta kuin aspiraatio-menetelmällä annettuina. Hengitettyinä neulamaisten hiilinanoputkien aikaansaama tulehdus muistutti suuresti allergista astmaa, mikä on poikkeuksellista. Neulamaiset hiilinanoputket aiheuttivat myös DNA-vaurioita keuhkosoluissa sekä aspiraatio-tekniikalla annosteltuina että hengitettyinä. Selvä perimämyrkyllinen vaikutus nähtiin hengitysilman kautta tapahtuneessa altistuksessa keuhkon huuhtelunäytteen soluissa (pääosin makrofageja). Hiilinanoputkien genotoksinen vaikutus oli paikallinen – muutoksia ei nähty verisoluissa. Pitkät, neulamaiset hiilinanoputket aiheuttivat DNA-vaurioita myös epiteelisolujen viljelmissä. Pitkät, taipuisat hiilinanoputket eivät olleet genotoksisia hiirillä, ja viljellyissä keuhkoputkiepiteelisoluissakin niiden vaikutus oli lievä. Tutkimuksemme vahvisti käsitystä pitkien ja neulamaisten hiilinanoputkien vaarallisuudesta ja toivat esiin aivan uusia vaikutuksia kuten astmaa muistuttavan tulehduksen syntyminen ja DNA-vauriot keuhkoissa. Pitkien hiilinanoputkien jäykkyys on ilmeisesti keskeinen tekijä niiden vaikutusten kannalta. Yli 50 nm paksut, jäykät, neulamaiset hiilinanoputket aiheuttivat voimakkaan tulehduksen ja olivat genotoksisia, mutta ohuemmilla (8-15 nm) ja taipuisilla hiilinanoputkilla ei juuri ollut vaikutuksia. Näyttää siltä, että pitkiä, neulamaisia hiilinanoputkia tulisi käsitellä erityistä varovaisuutta noudattaen.

TABLE OF CONTENTS

1 INTRODUCTION

1.1 Importance of engineered nanomaterials for economy and society

Engineered nanomaterials (ENM) have been defined as having at least one dimension ≤100 nm. In general, ENMs can be categorised into carbon-based materials, such as fullerenes and carbon nanotubes, other organic materials (e.g. nanocellulose, synthetic polymers), and inorganic nanoparticles, including nanosized metal oxides (zinc oxide, iron oxide, titanium dioxide, and cerium oxide, etc), metals (gold, silver and iron) and quantum dots (cadmium sulfide and cadmium selenide).

ENMs have attracted a great deal of attention during recent years, due to their many technologically interesting properties. The unique properties of ENM and their applications have given birth to large technological and economic growth, and future expectations for industries using materials at nano-scale. Nanotechnologies utilizing ENM are envisaged to become the cornerstone for a number of industrial sectors, such as micro-electronics, materials, paper, textile, energy, and cosmetics, which are all capable of incorporating some nano-scale-enabled properties into their goods, with an estimated annual turnover of ENM-based products of 3 trillion US dollars (Roco *et al*., 2010) by 2020.

ENM can be found in more than 800 consumer products (Woodrow Wilson International Centre for Scholars, 2011), including electronic components, cosmetics, cigarette filters, antimicrobial and stain-resistant fabrics and sprays, sunscreens, cleaning products, ski waxes, different surfaces requiring antimicrobial properties, and self-cleaning windows.

Nanotechnology applications are very likely to contribute positively to the quality of life through the production of durable and light materials, cleaner energy, and inexpensive clean water production, as well as by enabling several beneficial medical applications, especially smart drugs (Adlakha-Hutcheon *et al*., 2009). Additionally, great environmental benefits are predicted from nanotechnology related applications because of the savings in raw materials, the consumption of natural resources, and a reduced environmental pollution (Kuhlbusch *et al*., 2009).

It should be noted, however, that some of the properties that make ENM so unique and beneficial for technological applications may also endanger human health through the potential induction of cytotoxic effects, inflammation, and even cancer. These features include a large surface area to mass ratio, increased surface reactivity, altered physico-chemical properties such as changes in melting point or solubility, electrical conductivity, or changes e.g. in the crystalline structure of the materials (Maynard and Aitken, 2007; Elder, 2009).

1.2 Carbon nanomaterials

Carbon nanotubes, fullerenes, and mesoporous carbon structures constitute a new class of carbon nanomaterials with properties that differ significantly from other forms of carbon such as graphite and diamond. The ability to customize synthesized nanotubes by attached functional groups or to assemble fullerene clusters into three-dimensional arrays has opened up new avenues to design high surface area catalyst supports and materials with high photochemical and electrochemical activity. Carbon nanotubes are also the strongest and stiffest materials yet discovered in terms of tensile strength and elastic modulus, respectively. Some of the applications utilizing carbon nanotubes and fullerenes include semiconductors, controlled drug delivery/release, batteries, data storage, waste recycling, and thermal protection (De Volder *et al.*, 2013).

Fullerenes are spherical, caged molecules with carbon atoms located at the corner of a polyhedral structure consisting of pentagons and hexagons. The best known and most stable fullerene is C60. The discovery of fullerenes by laser vaporization technique resulted in awarding the 1996 Nobel Prize in Chemistry to Curl, Kroto, and Smalley.

Conventional **carbon nanotubes** (CNTs) are made of seamless cylinders of hexagonal carbon networks and are synthesized as single-wall (SWCNTs) or multiwall carbon nanotubes (MWCNTs). Electric field alignment is a powerful technique that has been shown to orient carbon nanotubes along a particular direction during the nanotube growth process. In addition, carbon nanotubes can be assembled as linear bundles in suspension, by applying a DC electric field. Individual nanotubes have extensively been studied for application in field emission devices.

Carbon nanobuds form a material which combines two previously discovered nanomaterials: CNTs and fullerenes (Nasibulin *et al*., 2007). In this new material, fullerenes are covalently bonded to the outer sidewalls of the underlying nanotube. Consequently, nanobuds exhibit properties of both CNTs and fullerenes. The characteristics of nanobuds suggest that they may possess advantageous properties compared with SWCNTs or fullerenes alone or in their non-bonded configurations.

1.3 Inflammatory and carcinogenic effects of carbon nanomaterials

Although the health effects of various carbon nanomaterials are poorly known at the moment, existing evidence suggests that exposure to certain MWCNTs has the capacity to induce severe adverse effects in rodent models. This underlines the need for further research and great caution before introducing such products into the market. The needle-like shape of certain CNTs has been compared with asbestos, raising concern that the widespread use of such CNTs may lead to pleural fibrosis or mesothelioma (cancer of the lining of the lung) which are mostly caused by exposure to asbestos.

It was recently reported that exposing the mesothelial lining of the body cavity of mice, as a surrogate for the mesothelial lining of the chest cavity, to long MWCNTs results in asbestos-like inflammatory behaviour. This included the formation of inflammatory lesions known as granulomas (Poland *et al*., 2008). Moreover, Takagi *et al*. (2008) exposed a tumor-prone p53+/- mouse strain via single intraperitoneal injection to crocidolite asbestos or MWCNTs and observed that the ability of MWCNTs to induce mesotheliomas in this mouse model markedly exceeded that of crocidolite asbestos. The induction of mesothelioma by MWCNTs was subsequently shown to be dose-dependent (Takagi *et al*., 2012). Another study by Sakamoto *et al*. (2009) reported that single intra-scrotal dose of MWCNTs in Fisher rats had a much higher potential to induce mesotheliomas than a comparable dose of crocidolite asbestos. Ryman-Rasmussen (2009) showed that MWCNTs reach the subpleura in mice after inhalation exposure. Subpleural fibrosis unique to this form of nanotubes increased after 2 and 6 weeks following inhalation - none of these effects was seen in mice that inhaled non-fibrous carbon black.

These observations merit immediate attention and need to be confirmed by other studies as they have a very remarkable impact on the risk assessment of these unique

nanomaterials. Moreover, the molecular mechanisms of observed pathologic phenomena need to be elucidated.

1.4 Genotoxic effects of carbon nanomaterials

Damage to DNA is one of the most significant human health hazards, since it results in mutations, chromosome alterations, and increased genetic instability which are associated with cancer development (Bonassi *et al*., 2010; Kisin *et al*., 2011). Most known human carcinogens are genotoxic (Waters *et al*., 2010). Carcinogenesis by carbon nanomaterials may also involve genotoxic processes. In principle, the possible genotoxicity of nanomaterials may result from primary or secondary mechanisms (Schins and Knaapen, 2007). Primary genotoxicity refers to the elicitation of genetic damage in the absence of inflammation, either by a direct interaction with genomic DNA or associated components that determine its integrity, or indirectly through the enhanced production of reactive oxygen species (ROS) by cellular constituents in response to their interaction with particles or through the depletion of antioxidants within the cell (Donaldson *et al*., 2010). Secondary genotoxicity is probably also an oxidative stress-driven response, but in this case the oxidants are considered to be derived from inflammatory leucocytes recruited to the site of particle deposition (Donaldson *et al*., 2010).

It has been suggested that the apparent clastogenic (chromosome-breaking) capacity of various fibrous materials, such as asbestos, CNTs, and carbon nanofibers, is linked to the presence of fiber-associated iron, which would initiate ROS generation via a Fenton reaction (Kisin *et al*., 2011; Catalán *et al*., 2011). Fibrous materials have also been reported to exhibit aneugenic effects (induction of numerical chromosome alterations). CNTs (Muller *et al*., 2008, Sargent *et al*., 2010, 2012), carbon nanofibers (Kisin *et al*., 2011), and crocidolite asbestos (Yegles *et al*., 1995; Dopp *et al*., 1997) induced chromosomal aneuploidy and disturbed the mitotic spindle. The similarities of SWCNTs with microtubules has been suggested to make it possible for thin nanotubes to be incorporated into cellular structures including the mitotic spindle, which could result in the disruption of the centrosome and microtubules (Sargent *et al*., 2010, 2012), whereas physical interference with the spindle might occur with larger fibers such as asbestos (Cortez and Machado-Santelli, 2008). In both cases, the inhibition of the separation of dividing cells induces multi-polar mitotic spindles, which results in errors of chromosome number (Sargent *et al*., 2010, 2012). The length of the fibers could differentially affect

their aneugenic capacity. In fact, long asbestos fibers were more genotoxic and carcinogenic than shorter fibers (Cortez and Machado-Santelli, 2008). Similarly, high-aspect-ratio MWCNTs exhibited higher toxicity than low-aspect-ratio MWCNTs (Kim *et al*., 2011).

2 AIMS OF THE STUDY

The aims of this study were to evaluate whether CNTs cause inflammatory and genotoxic effects.

The specific goals of the final project were to investigate:

Inflammatory reactions in the lungs of mice following CNT exposure. This research was expected to produce new information on inflammatory changes caused by CNTs in comparison with asbestos exposure. In addition, correlation between *in vivo* and *in vitro* approaches was investigated to gain insight on inflammatory mechanisms elicited by CNTs.

Genotoxicity of CNT exposure to mouse lungs. This research focused on assessing possible DNA damage and chromosomal changes caused by CNTs. In addition, correlation between *in vivo* and *in vitro* results was investigated to shed light on the genotoxic mechanisms of CNTs.

The original project proposal additionally included plans to study (a) the importance of inflammation in CNT-induced cancer and (b) exposure to CNTs at workplaces. Due to cuts in the budget of the project, this research was not included in the final project. However, occupational exposure to nanomaterials (including carbon nanotubes) is studied in another, on-going project (No. 112132) supported by the Finnish Work Environment Fund.

3 MATERIALS AND METHODS

3.1 Carbon nanotubes and their characterisation

Four different carbon nanomaterials and asbestos were selected for the *in vitro* -experiments (see also Table 1):

1. Carbon black (Average size 14 nm; Printex 90®, Evonik Industries)
2. Short MWCNTs (Outer diameter, OD, 5-20 nm, length 1- >10 µm; Baytubes C 150 HP, Bayer Material Science)
3. Long tangled MWCNTs (OD 8-15 nm, length 10-50 µm; MWCNTs 8-15 OD, CheapTubes Inc©)
4. Long needle-like MWCNTs (OD >50 nm, length 13 µm; Mitsui-7, Mitsui & Co.)
5. Crocidolite asbestos (Average diameter 180 nm, length 4.6 µm; Pneumoconiosis Research Centre)

The size and morphology of the nanomaterials were characterised by scanning (SEM) and transmission (TEM) electron microscopy (Zeiss ULTRAplus FEG-SEM, Carl Zeiss NTS GmbH, Germany and FEI Quanta 200F SEM FEI Company, The Netherlands and Jeol JEM 2010 TEM, Jeol Ltd., Japan) and their composition by energy dispersive spectroscopy (EDSThermoNoran Vantage, Thermo Scientific, the Netherlands attached to Jeol JEM 2010 TEM) (Table 1 and Fig. 1).

Two MWCNTs of different appearances were chosen to be tested *in vivo.*

1. Long tangled MWCNTs (outside diameter 8-15 nm, length 10-50 µm; CheapTubes Inc©)
2. Long needle-like MWCNTs (outside diameter >50 nm, length 13 µm; Mitsui-7; Mitsui & Co.)

Table 1. Characteristics of the nanomaterials and crodicolite asbestos used (see also Fig. 1).

Variable	Short MWCNTs	Long tangled MWCNTs	Long needle-like MWCNTs	Carbon black	Asbestos
Trade name	Baytubes C150 HP	MWCNT 8-15 nm	Mitsui MWCNT-7	Printex 90®	Crocidolite asbestos
Manufacturer	Bayer Material Science	Cheaptubes, Inc.	Mitsui & Co. Ltd	Evonik Industries	Pneumoco-niosis Research Centre
Characteristics of primary fibres or particles (provided by manufacturer)	OD 2-20 nm Length 1->10 µm	OD 8-15 nm Length 10-50 µm SSA 233 m^2/g	OD >50 nm Length ~13 µm	Average size 14 nm SSA 300 m^2/g	ø 180 nm Length 4.6 µm
Composition measured by TEM + EDS, average of 5 measurements	Carbon content >99 % (w/w) Residual catalyst metals: Co <0.2 % (w/w)	Carbon content >99 % (w/w) Residual catalyst metals: Co, Fe, Ni <0.5 % (w/w)	Carbon content >99 % (w/w) Residual catalyst metals: < 0.1 % (w/w; detection limit)	Carbon content ~ 100 % (w/w)	Not applicable

Compositional analysis shown is the average of five separate analyses by transmission electron microscopy (TEM) and energy dispersive X-ray spectroscopy (EDS). MWCNTs, multi-walled carbon nanotubes; OD, outer diameter; SSA, specific surface area.

In addition, the nanomaterials were compared to crocidolite asbestos (PRC, South-Africa) as a positive control. These materials were chosen in light of existing knowledge on the induction of mesothelioma and inflammation by MWCNTs (Poland *et al*., 2009; Takagi *et al*., 2008; Sakamoto *et al*., 2009). An important point was also the fact that MWCNTs have presently far greater industrial importance than SWCNTs, which makes it more likely for employees to be exposed to MWCNTs than SWCNTs.

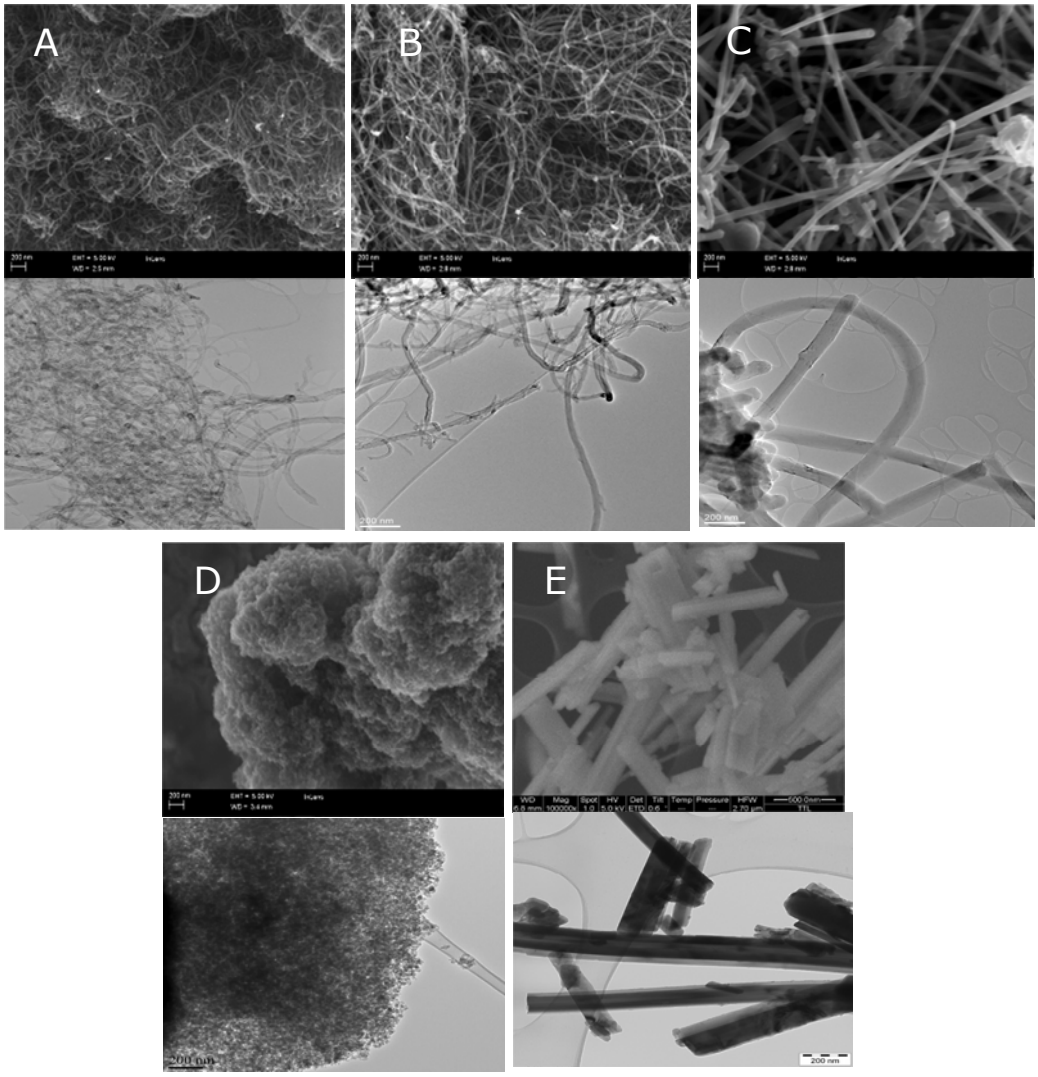

Figure 1. The morphology of the test materials, as studied by scanning electron microscopy (SEM; upper part of each micrograph pair) and transmission electron microscopy (TEM; lower part of each micrograph pair). A , short multiwalled carbon nanotubes (MWCNTs). B, long tangled MWCNTs. C, long needle-like MWCNTs. D, carbon black. E, crocidolite asbestos.

3.2 *In vitro* studies

3.2.1 Immunotoxicological studies

In vitro immunotoxicological studies were performed using human monocyte-derived primary macrophages. Primary macrophages were exposed to different carbon nanomaterials (carbon black, short MWCNTs, long tangled MWCNTs, long needle-like MWCNTs) and crocidolite asbestos at two different concentrations (10 and 100 µg/ml). The characteristics of the materials used are represented in Table 1 and Fig. 2. The secretion of important pro-inflammatory cytokines IL-1α and IL-1β after exposure to the carbon nanomaterials and asbestos was studied by the ELISA assay. To investigate whether an important molecular complex, NLRP3 inflammasome, previously associated with particulate exposure (e.g. asbestos, silica) is activated, macrophages were left untreated or pre-treated with bacterial lipopolysaccharide (LPS, 100 ng/ml) before the exposure. All studies were performed using a 6-h exposure, and the secretion of pro-inflammatory cytokines caused by long needle-like MWCNTs was also studied after 3-h and 9-h exposures to find out the dynamics of cytokine secretion.

Cells: Peripheral blood mononuclear cells (PBMCs) from healthy blood donors (Finnish Red Cross Blood Transfusion Service, Helsinki, Finland) were isolated from buffy coats by low-speed density gradient centrifugation on Ficoll-Paque Plus (Amersham Biosciences, Uppsala, Sweden). The monocytes were resuspended in RPMI-1640 (Invitrogen, Paisley, UK) with supplemental 1 % penicillin-streptomycin (PEST; Invitrogen, Paisley, UK) and 1 % L-glutamine (Ultraglutamine®; Invitrogen, Paisley, UK). After 45 min of attachment on 6- or 12-well-plates, non-adherent cells were washed away with Dulbecco's phosphate buffered saline without Ca^{2+} and Mg^{2+} (DPBS; Lonza, Basel, Switzerland). The adherent monocytes were cultured in serum-free macrophage medium (Macrophage-SFM; Invitrogen, Paisley, UK) supplemented with granulocyte-macrophage colony-stimulating factor (GM-CSF; BioSource, Camarillo, CA, USA) and PEST. The cells were cultured for 7 days in the respective medium to allow for differentiation of the macrophages before exposure to the nanomaterials.

Dispersion preparation for* in vitro *experiments: Nanomaterial suspensions for the experiments were prepared by weighing the materials into glass tubes and

diluting them to a stock dispersion of 1 000 µg/ml with 2 % fetal bovine serum (FBS) in phosphate buffered saline (PBS) which was sonicated for 20 min at 30 °C. The stock dispersion was further serially diluted to 100 and 10 µg/ml final concentrations in serum-free macrophage medium and sonicated for 20 min at 30 °C just before cell exposures. Old media was carefully removed and replaced with new media containing the final concentrations of nanomaterials.

Electron microscopy: PBMCs were isolated and purified as described above. After 7 days of differentiation, the cells were primed for 2 h with LPS and exposed to different carbon nanomaterials and asbestos. After the exposure, the cells were washed twice with DPBS, fixed with 2.5 % glutaraldehyde in 0.1 M phosphate buffer, and removed from the plate by scraping. The cells were post-fixed in 1 % osmium tetroxide, dehydrated and embedded in Epon LX-112 (Ladd Research, Williston, VT, USA). Thin sections were collected on uncoated copper grids, stained with uranyl acetate and lead citrate and then examined with a transmission electron microscope operated at an acceleration voltage of 80 KV (JEM-1220, Jeol Ltd., Japan).

Reagents: Bacterial LPS (*Escherichia coli* 0111:B4, Sigma-Aldrich, Germany) was used at a concentration of 100 ng/ml. Pharmacological inhibitors used in the experiments were cathepsin B inhibitor Ca-047-Me (10 µM; Calbiochem, Germany) and $P2X_7$ receptor inhibitor AZ11645373 (1 µM; Sigma-Aldrich). When inhibitors were used, they were added to the wells 1 h prior to exposure to the materials.

Small interfering RNA assays: After 6 days of cell culture in 12-well plates, macrophages were transfected with 200 nM non-targeting control small interfering RNA (siRNA, AllStars Negative Control siRNA, Qiagen, CA, US), 50 nM of four different NLRP3 siRNAs (Hs_CIAS1_6, Hs_CIAS1_9; Hs_CIAS1_10, Hs_CIAS1_11; Qiagen) or 100 nM of two different $P2X_7$ siRNAs (Hs_P2RX7_1, Hs_P2RX7_2; Qiagen) using the HiPerFect Transfection Reagent (Qiagen) according to the manufacturer's instruction. After 4 h of incubation with siRNAs, cell culture media was removed and 500 µl of fresh media was added to the wells. On day 7, appropriate wells were primed for 2 h with 100 ng/ml of LPS, and the cells were left untreated or treated with 100 µg/ml of long needle-like MWCNTs or asbestos. After the exposure period, cell culture supernatants were collected.

Western blotting and ELISA: Processing and secretion of IL-1β, cathepsin B and ASC were analysed by Western blot performed by using concentrated cell supernatants. Cell culture supernatants (6 ml) were concentrated by Amicon UItra-15 –centrifugal filter devices (Millipore, MA, US) according to the manufacturer's instructions. After the concentration, 30 µl from 240 µl of each supernatant was separated on 12 % SDS-PAGE at 200 V and transferred onto Immobilon-P Transfer Membranes (Millipore, MA, US) by the Isophor electrotransfer apparatus PowerPac Basic (Bio-Rad Laboratories) at 4 ºC and 100 V for 1 h. The membranes were blocked in PBS containing 5 % non-fat milk for 30 min after which they were incubated at 4 ºC overnight with primary antibodies. After this, the membranes were incubated at room temperature for 1 h with the appropriate HRP-conjugated secondary antibodies (Dako A/S, Denmark). Finally, proteins were visualised by the Image Quant LAS 4000 mini quantitative imager (GE Healthcare, CT, US). Anti-IL-1β antibody has previously been described (Palomäki *et al*., 2011), anti-Cathepsin B antibody was purchased from Calbiochem and anti-ASC antibody from Millipore. Both human IL-1α MAX^{TM} Deluxe and IL-1β Eli-pair were purchased from Diaclone (Besançor Cedex, France) and human IL-18 ELISA from Bender MedSystems (Bender MedSystems, Austria). All ELISAs were performed according to the manufacturer's instructions.

Statistical analyses: Each macrophage sample represented a pool of separately stimulated cells from three different blood donors. ELISA results were combined from values obtained in three different stimulations, and Western blot results were representative of three independent, but similarly performed experiments unless otherwise mentioned. Data were analysed using GraphPad Prism 4 Software (GraphPad Software Inc., San Diego, CA, USA). An unpaired *t*-test or Mann-Whitney *U*-test was used to compare the differences between the groups. A P-value of <0.05 was considered to be statistically significant. In ELISA figures, data were expressed as means ±SD.

3.2.2 Genotoxicological studies

Dispersion preparation for* in vitro *experiments: The materials were dispersed in BEGM cell culture medium (Clonetics, Walkerwille, MD, USA) supplemented with 0.6 mg/ml of BSA (bovine serum albumin) and subjected to ultrasonication (Elmasonic, Singen, Germany) for 20 min at 37 kHz prior to addition to the cell

cultures. Both the stock dispersions and the serially diluted final dispersions were sonicated.

Cell culture: Transformed human bronchial epithelial BEAS 2B cells, exhibiting an epithelial phenotype (Reddel *et al*., 1988) were obtained from the American Type Culture Collection through LGC Promochem AB (Borås, Sweden). The BEAS 2B cells were grown in serum-free BEGM medium at 37 ºC in a humidified atmosphere of 5 % CO_2. For assays on cytotoxicity and DNA damage (the comet assay), 20 000 log-phase BEAS 2B cells were plated on each well of a 24-well plate (Nunc, Roskilde, Denmark; culture area 1.9 cm^2/well, 1 ml culture medium per well) two days prior to exposure. For the micronucleus (MN) assay, 250 000 cells were grown on T25 culture flasks (Nunc, Roskilde, Denmark; culture area 25 cm^2/ flask, 5 ml culture medium per flask) for three days prior to exposure, i.e. until semiconfluency.

Cytotoxicity: Semiconfluent cells on 24-well plates were exposed to 500 µl per well of ultrasonicated dispersions of carbon nanomaterials for 4, 24 and 48 h at doses 5, 10, 50, 80, 100, 200, 250, 300 and 350 µg/cm^2 (corresponding to 9.5, 19, 95, 152, 190, 380, 475, 570 and 665 µg/ml). Untreated controls were included at each time point. All the treatments were done in duplicate and the experiments were repeated twice.

Cytotoxicity was measured after collecting the cells by trypsination. In the Trypan blue dye exclusion technique, the number of living (unstained) cells was determined under a phase-contrast microscope. In the CellTiter-Glo® Luminescent Cell Viability Assay (Promega, Madison, USA), the number of viable cells was based on the quantification of ATP which signals the presence of metabolically active cells. Cell number was expressed as the percentage of viable cells in the treated cultures in comparison with the control cultures. These assays reflect all treatment-related effects (necrosis, cell cycle delay and apoptosis) that reduce the number of viable cells.

Comet assay: The single cell gel electrophoresis (comet) assay was used to study DNA strand breaks and alkaline labile sites in BEAS 2B cells after nanomaterial exposures. Semiconfluent cultures on 24-well plates were exposed (500 µl per well) for 4 and 24 h to six doses of the carbon nanomaterials: 5, 10, 50, 100, 200 and 250 µg/cm^2 (corresponding to 19, 38, 190, 380, 760 and 950 µg/ml, respectively). The doses were chosen according to the Trypan blue cytotoxicity assay. Untreated controls and positive controls (20 mM hydrogen peroxide, Riedel-de Haen, Seelze, Germany) were included in all series.

The comet assay was performed at alkaline conditions (pH > 13) as described previously (Nygren *et al.*, 2004). Briefly, after the exposure the cells were trypsinised and centrifuged at 1100 rpm for 5 min. Ten to thirty thousand cells were resuspended in 75 µl molten (37 °C) 0.5 % low-melting-point agarose (LMPA; Merck, Darmstadt, Germany). The resuspended cells in agarose were applied to dry microscope slides (Menzel Gmbh, Braunschweig Germany), pre-coated with 1 % normal-melting agarose (BDH Electran VWR international Ltd., Lutterworth, UK), and the agar was allowed to solidify for 10 min. The slides were thereafter immersed in cold lysing solution (2.5 M NaCl, 100 mM EDTA, 10 mM Tris, 1 % Triton X-100) for at least 1 h at 4 °C, after which they were transferred to an electrophoresis tank containing freshly made electrophoresis buffer (1 mM EDTA, 300 mM NaOH; pH> 13), where they were kept for 20 min at room temperature to allow DNA unwinding. Electrophoresis was performed in the same buffer at room temperature for 15 min at 24 V and 300 mA (0.8 V/cm). The slides were then neutralized three times with 0.4 M Tris buffer (pH 7.5), air-dried, and fixed in methanol. DNA was stained with ethidium bromide (2 µg/ml) in water for 5 min.

The slides were coded, and one scorer performed the comet analysis using a fluorescence microscope (Axioplan 2, Zeiss, Jena, Germany) and an interactive automated comet counter (Komet 5.5, Kinetic Imaging Ltd., Liverpool, UK). The percentage of DNA in the comet tail from 100 cells per replicate was used as a measure of the amount of DNA damage. In each experiment, two replicates per dose were included, and the experiment was repeated twice.

Micronucleus assay: Semiconfluent cells in T25 flasks were exposed for 48 h to five doses of long tangled MWCNTs (Cheaptubes): 5, 10, 50, 100 and 200 µg/cm^2 (corresponding to 25, 50, 250, 500 and 1000 µg/ml) and to five doses of long needle-like MWCNTs (Mitsui-7): 2.5, 5, 10, 20 and 40 µg/cm^2 (corresponding to 12.5, 25, 50, 100 and 200 µg/ml). The doses were chosen based on the Trypan blue cytotoxicity assay. Cytochalasin B (Cyt-B; 9 µg/ml; Sigma-Aldrich Chemie, Steinheim, Germany) was added to the cell cultures after 6 h of exposure to induce binucleation of dividing cells. Untreated controls and positive controls receiving 150 ng/ml mitomycin C (MMC; Sigma-Aldrich, Steinheim, Germany) were also included.

After the exposure, the cells were trypsinised for 20 min, PBS containing 10 % FBS was added, and the cells were centrifuged at 1,100 rpm for 5 min. The supernatant was

removed, and PBS was added to the cell suspension. After centrifugation and removal of the supernatant, the cells were incubated in 5 ml of hypotonic solution (50 % RPMI) for <2 min. The cells were again centrifuged and first fixed in 3:1 methanol-acetic acid and then in 97 % methanol - 3 % acetic acid. The cells were spread on microscopy slides and left to dry overnight. The slides were stained with acridine orange (32 µg/ml in Sørensen buffer, pH 6.8) for 1 min and rinsed in Sørensen buffer for 3 x 3 min. Finally, the slides were stained with 4',6-diamidino-2-phenylindole (DAPI, 5 µg/ml) for 5 min, rinsed in tap water and allowed to dry. The stained and fixed slides were kept protected from light at 4 ºC until analysis.

The slides were coded, and the frequency of micronucleated cells in 2000 binucleate cells (1000 cells/repeat) were analysed by one scorer using an Axioplan 2E Universal microscope (Zeiss, Jena, Germany). Binucleate cells were identified with 40× magnification using a green/red (FITC/TRITC) double filter. MN in the cells were verified with a DAPI filter to ensure DNA content.

Cytokinesis block proliferation index (CBPI; Surrallés *et al*., 1995) was calculated from 200 cells per culture as follows: CBPI = [(No. mononucleate cells) + 2(No. binucleate cells) + 3(No. multinucleate cells)]/(Total No. cells).

Statistics: Two-way or one-way analyses of variance (ANOVA) were applied, respectively, to examine whether the percentage of DNA in tail (Comet) or the frequency of micronucleated cells and the CBPI values were statistically significantly affected by the *in vitro* exposure to the CNTs in comparison with the untreated control cultures. Since differences among experiments have previously been reported for the Comet assay, "experiment" was included as a second factor (in addition to nanoparticle dose) in the ANOVAs, to reduce the residual variability of the model. Tukey's test was applied for an *a posteriori* comparison of the means.

For all the assays, linear regression analysis was applied to examine whether a linear dose-response could be observed. The difference between the positive control and the untreated control was assessed by a two-sample *t*-test. Differences were interpreted to be significant if the *p*-value was <0.05. All statistical analyses were performed with the Statistix for Windows 2.0 program (Tallahassee, USA).

3.3 *In vivo* studies

Animals: Female C57Bl/6 mice (7-8 weeks old) were purchased from Scanbur AB (Sollentuna, Sweden) and quarantined for one week. The mice were housed in groups of four in stainless steel cages bedded with aspen chip and were provided standard mouse chow diet (Altromin No. 1314 FORTI, Altromin Spezialfutter GmbH & Co., Germany) and tap water *ad libitum*. The environment of the animal room was carefully controlled, with a 12-h dark/light cycle, temperature of 20-21 °C, and relative humidity of 40-45 %.

The experiments were performed in agreement with the European Convention for the Protection of Vertebrate Animals Used for Experimental and Other Scientific Purposes (Strasbourg March 18, 1986, adopted in Finland May 31, 1990). The study was approved by the Animal Experiment Board and the State Provincial Office of Southern Finland.

Inhalation: The fibrous materials were aerosolized with a fluid bed aerosol generator (TSI FBAG 3400A) which produced constant aerosol into the exposure chamber. The aerosol in the chamber was monitored using a variety of equipment: mass concentration with weighted filter capsules, number concentration with a condensation particle counter, and size distribution with an optical particle sizer.

After performing the first inhalation study (Fig. 2) with fibrous materials, we came to the conclusion that our facilities need upgrading to ensure the safety of the researchers. This lead to extensive planning and renovations in our exposure facilities. The generator and the exposure chamber were encapsulated (Fig. 3). The spread of the study material was restrained as well as possible. We also developed strict working procedures and applied the best possible personal protection for our workers. The facilities were ready for use during the last few months of the project. Planning and executing the needed changes was a valuable learning experience which was used as an example of a model solution for possible ENM exposures.

In the summer of 2011, we performed our first study in the new facilities. We exposed 8 mice to long needle-like MWCNTs for 4 hours during one day and during 4 consecutive days. The exposure concentration was kept constant at ~8 mg/m³. Samples were collected from the mice 24 h after the end of the exposure for immunotoxicological studies in the 1-day experiment and for both immunotoxicological and genotoxicological analyses, using the same animals, in the 4-day experiment.

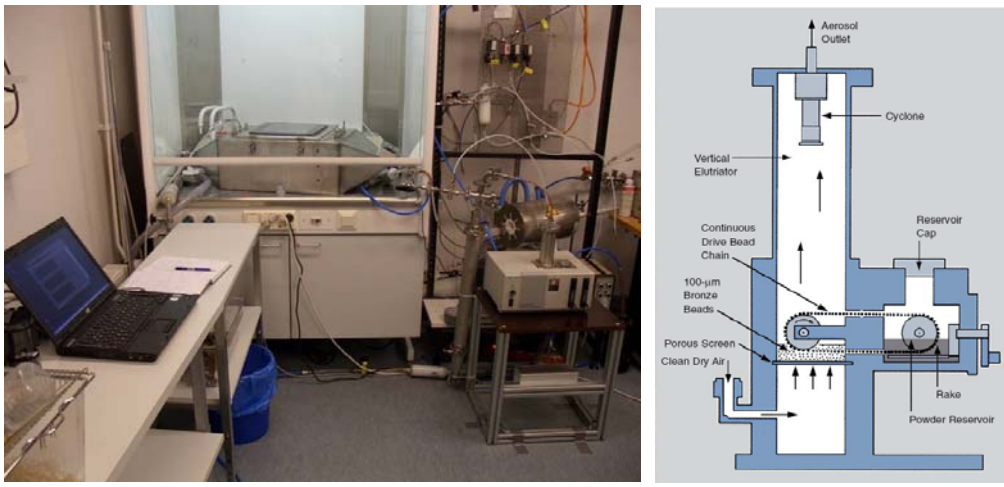

Figure 2. Old exposure facilities (left) and a schematic drawing of the fluidized bed aerosol generator (right).

Pharyngeal aspiration: Pharyngeal aspiration is a safe and reliable method to use for exposure of dusting, dangerous or very expensive materials. The study material was suspended in PBS containing 0.6 mg/ml BSA and sonicated for 20 min. The mice were anesthetized with vaporized 4.5 % isoflurane and suspended by their incisors on a thin wire on a custom made mouse support at approximately 66 degrees angle. A cold-light source was placed against their throat to provide optimal illumination of the trachea. The tongue was pulled out using blunted forceps and pressed down using a small spatula to prevent the mouse from swallowing. 50 µl of the particulate suspension was delivered onto the vocal folds under visual control using an extended pipette tip (Finntip 200 Ext). Immediately after delivery the mouse nostrils were covered enforcing the mouse to inspire the instilled suspension.

Figure 3. New exposure facilities and personal protection.

The pharyngeal aspiration method was adapted to our institute to expose mice with during the renovations in the inhalation exposure facilities. Female C57Bl/6J-mice (6-8 mice per group) were exposed to the study material using a single pharyngeal aspiration exposure.

3.3.1 Immunotoxicological studies

Exposure protocol: In single exposures by pharyngeal aspiration, we used a MWCNT dose of 10 µg per mouse (50 µl of a 0.2 mg/ml dispersion) and for the 28-day exposure we used 10 µg and 40 µg (50 µl of a 0.8 mg/ml dispersion) MWCNTs per mouse. The mice were sacrificed 4 and 16 h or 28 days after the exposure, and samples were collected. The inhalation exposure protocol has been described above.

Antagonists: For the antagonist experiment (Table 2), we first gave i.p injections and after 16 h performed pharyngeal aspiration. The animals were sacrificed 4 h after the aspiration exposure. PBS containing 0.6 mg/ml BSA and 10 µg of long needle-like MWCNTs (Mitsui-7) was given per mouse (0.2 mg/ml dispersion) and the antagonists anakinra (Kineret; Biovitrum AB, Stockholm, Sweden) and etanercept (Enbrel; Wyeth Pharmaceuticals, Hampshire, UK) 200 µg/mouse both times.

Sample collection: The mice were sacrificed using an overdose of isoflurane. Blood was collected from the *vena cava* (hepatic vein), and the lungs were lavaged with PBS (800 µl for 10 s) via the tracheal tube. The bronchoalveolar lavage (BAL) sample was cyto-centrifuged on a slide, and the cells were stained with May Grünwald-Giemsa (MGG) and

counted under light microscopy. The BAL supernatant was stored at -70 ºC for cytokine analysis, and the remaining cells were fixed in ethanol (1:2). The mouse chest was opened, and half of the left pulmonary lobe was removed, quick-frozen and kept at -70 ºC for later RNA isolation. A slice of the lungs and part of BAL cells were collected from the mice, fixed with glutaraldehyde and then prepared for electron microscopy. The rest of the lungs were formalin-fixed, embedded in paraffin, cut, affixed on slides, and stained with hematoxylin and eosin (H&E), periodic acid-Schiff (PAS), and Herovici's (HERO) solutions.

Table 2. Treatment groups included in the antagonist experiment with long needle-like multiwalled carbon nanotubes (MWCNTs; 10 µg/mouse). Etanercept (200 µg/mouse) was used as an antagonist of tumor necrosis factor alpha (TNF-α) and anakinra (200 µg/mouse) as an antagonist of interleukin 1 beta (IL-1β).

Intraperitoneal injection	**Pharyngeal aspiration**
PBS/BSA	PBS/BSA
PBS/BSA	PBS/BSA + long needle-like MWCNTs
PBS/BSA + etanercept	PBS/BSA + long needle-like MWCNTs + etanercept
PBS/BSA + anakinra	PBS/BSA + long needle-like MWCNTs + anakinra
PBS/BSA + etanercept + anakinra	PBS/BSA + long needle-like MWCNTs + etanercept + anakinra

BSA/PBS, bovine serum albumin (0.6 mg/ml) in phosphate-buffered saline.

RNA isolation from the lung tissues: The lung samples were homogenized in a FastPrep FP120 (BIO 101, Thermo Savant, Waltham, Mass. USA) -machine and RNA was extracted using the FastRNA Pro Green Kit (Qbiogene/ MP Biomedicals, Illkirch, France) and its instructions. The quantity and purity of extracted RNA was determined by NanoDrop spectrophotometer (ND-1000, Wilmington, Delaware USA). Isolated total RNA was dissolved in DEPC water and stored at -70ºC.

cDNA synthesis: cDNA was synthesized from 1 µg of total RNA in a 25 µl reaction using MultiScribe Reverse Transcriptase and random primers (The High-Capacity cDNA Archive Kit, Applied Biosystems, Foster City, CA) using the manufacturer's protocol. The synthesis was performed in a 2720 Thermal Cycler (Applied Biosystems, Carlsbad, California, USA) starting with 25 °C for 10 minutes and continuing with 37 °C for 120 minutes.

Polymerase chain reaction (PCR) amplification: PCR primers and probes were ordered as pre-developed assay reagents from Applied Biosystems. The real-time quantitative PCR was performed in a 96-well optical reaction plate with Relative Quantification 7500 Fast System (7500 Fast Real-Time PCR system, Applied Biosystems) using the manufacturer's instructions. Amplifications were done in 11 µl reaction volume containing 20 ng cDNA and TaqMan universal PCR master mix and primers provided by Applied Biosystems. Endogenous 18S was used as the housekeeping gene.

ELISA: Mouse ELISAs (eBioscience, San Diego, CA, US) were performed according to manufacturer's instructions. An ELISA plate absorbance reader (Multiskan MS, Labsystems, Titertek Multiscan, Eflab, Turku, Finland) was used to read the results.

Luminex: For analysis of proteins in BAL fluid supernatants we used a Milliplex Mouse Cytokine/Chemokine Immunoassay (Millipore Corporation, Billerica, MA) according to the manufacturers' protocol. 3 % bovine serum albumin (BSA; Sigma-Aldrich, St Louis, MO) in PBS was added at a concentration of 0.5 % to samples, controls and standards to ensure sufficient protein amounts for the assay. Assay was performed using Luminex xMAP Technology (Bio-Plex 200 System, BioRad, Hercules, CA).

Electron microscopy: Samples were fixed in 2.5 % glutaraldehyde and postfixed in 1 % osmium tetroxide, dehydrated and embedded in LX-112 (Ladd Research, Williston, VT, USA). Thin sections were collected on uncoated copper grids, stained with uranyl acetate and lead citrate and then examined with a transmission electron microscope operated at 100 KV (JEM-1220, Jeol Ltd., Tokyo, Japan).

Fibrosis: Lung fibrosis was analysed using Sircol Collagen Assay kit following the manufacturer's instructions. The HERO stained slides were analysed for possible fibrotic cells using light microscopy.

Statistical analyses: Data were analysed using GraphPad Prism 5 Software (GraphPad Software Inc., San Diego, CA, USA). An unpaired t-test or Mann-Whitney *U*-test was used to compare the differences between the groups. A P-value of <0.05 was considered to be statistically significant.

3.3.2 Genotoxicological studies

Exposure protocol: In each experiment performed by pharyngeal aspiration, six mice per group were exposed to a single dose of one of the following materials: a) first experiment: 1, 10 and 40 µg/mouse (respective dispersions: 0.02, 0.2 and 0.8 mg/ml) of long needle-like MWCNTs (Mitsui-7), b) second experiment: 50, 100 and 200 µg/mouse (respective dispersions: 1, 2 or 4 mg/ml) of long needle-like MWCNTs, and c) third experiment: 10, 40, 100 and 200 µg/mouse (respective dispersions: 0.2, 0.8, 2, and 4 mg/ml) of long tangled MWCNTs (Cheaptubes). In addition, in each experiment the negative control mice (n= 6) were exposed to 50 µl of the solvent alone (PBS with 6 % bovine serum albumin), whereas the positive control group (n = 6) received a single dose of 1 mg/mouse (20 mg/ml dispersion) of tungsten carbide-cobalt mixture (WC-Co; kindly provided by Dr. Lison, Université catholique de Louvain, Belgium).

The inhalation exposure protocol has been described above. As a positive control, we included a group of 8 mice simultaneously exposed to a single dose of WC-Co (1 mg/mouse) by pharyngeal aspiration, as described in the previous paragraph and to Mitomycin C (MMC, 2 mg/kg) by intraperitoneal injection.

Sample collection: The mice were sacrificed 24 h after the exposure using an overdose of isoflurane, and the samples were collected as previously described in the immuno-toxicological section, with small modifications. Briefly, blood was collected from the vena cava in an insuline syringe containing 0.04 ml EDTA, to prevent coagulation, placed into a tube and stored on ice. To obtain the BAL cells, the lungs were lavaged with 800 µl of PBS (BAL sample for the determination of cell composition), and then infused six times with 0.8 ml sterile 0.15 M NaCl through the trachea (BAL sample for the comet analyses). The first BAL sample was cytocentrifuged on a slide, and the cells were stained using MGG and counted under light microscopy. The second BAL fluid was stored on ice until centri-fugation at 400 x g for 5 min. The mouse chest was opened and the lungs were removed and placed, on ice, into a petri dish containing 0.15 M NaCl. The left lung (or the right lung in the inhalation experiment) was minced in chilled mincing solution (Hank's balanced salt solution with 20 mM EDTA) and mechanically dispersed into a single cell suspension by using a cell strain (40 µm Ø). Then, the cell suspension was collected, divided in two aliquots and stored on ice until centrifugation at 400 ×g for 5 min. In the pharyngeal aspiration experiments, the caudal lobule of the right lung was formalin-fixed, embedded in paraffin, cut, affixed on slides and stained with H&E, PAS and HERO solutions. The rest

of the right lung was quick-frozen and stored at -70 ºC for further possible analyses. From some few animals, the medium lobule of the right lung was fixed with glutaraldehyde and prepared for electron microscopy, as described in the immunological studies section. In addition, in the inhalation experiment, the femurs of the mice were collected to extract bone marrow cells.

Comet assay on BAL and lung suspensions: The comet assay was performed in alkaline conditions (pH > 13) as described above. The percentage of DNA in the comet tail from 100 cells per animal (two replicates, 50 cells each) was used as a measure of the amount of DNA damage.

γ-H2AX assay on peripheral blood mononuclear cells and lung cell suspensions: Peripheral blood was incubated in ice-cold lysis solution (0.154 M NH_4Cl, 0.01 M $KHCO_3$, 0.09 mM EDTA, pH 7.3) on ice for 10 min to remove erythrocytes. After centrifugation at 4000 rpm, 4 min at 4 °C, the cell pellet was twice resuspended in 10 ml of ice-cold lysis solution for 10 min and centrifuged as above. The cell pellet was suspended in 2 ml of cold PBS and stored on ice until processing onto slides.

Lung cell suspension was incubated in ice-cold 96 % ethyl alcohol, mixed carefully and washed twice with PBS. After the last centrifugation, the cell pellet was suspended in 0.5 ml of cold PBS and stored on ice until processing onto slides.

Blood and lung suspensions were directly spun onto polylysine slides with a cytocentrifuge (Shandon Cytospin 2, Astmoor, UK). The slides were then fixed with freshly prepared 4 % paraformaldehyde at 4 °C for 25 min. The cells were rinsed three times in PBS and made permeable by incubation in 0.5 % Triton X-100 in PBS for 5 min at room temperature. Nonspecific antibody binding was blocked by incubation in 5 % foetal calf serum in PBS for 1 h. The cells were then incubated with 1:50 dilution of Phospho-Histone H2A.X (Ser139) (20E3) Rabbit mAb (Alexa fluor 488 conjugated) (Cell Signaling) in 1 % BSA in PBS. After overnight incubation at 4 °C, the slides were washed three times with PBS and counter-stained with 4,6-diamidino-2-phenylindole (DAPI, 1 µg/ml) for 5 min. Then, the slides were rinsed in tap water and allowed to dry. Immediately before analysis, the slides were mounted in Prolong Gold antifade reagent (Invitrogen) and mounted with a cover slip. The slides were coded, and the frequency of cells with more than four distinct foci in the nucleus (positive cells) in 1000 mononucleate cells per animal and per tissue was scored by one microscopist using an Axioplan 2E Universal microscope (Zeiss, Jena, Germany).

The presence of γ-H2AX-foci is a measure of DNA double-strand breaks.γ-H2AX is the phosphorylated form of histone 2AX. H2AX becomes phosphorylated on serine 139 as a reaction on DNA double-strand breaks.

Automated micronucleus assay in bone marrow erythrocytes: Bone marrow extraction and preparation of the slides for automated MN analysis were done primarily as previously described by Romagna *et al*. (1989). Briefly, one femur was removed from each mouse, cut at the proximal end of the bone and flushed with a foetal bovine serum mix (FBS in 25 mM EDTA) to collect bone marrow cells in suspension. The suspension was loaded into Poly-prep chromatography columns (0.8 x 4 cm) that contained a 30-µm pore size filter bed (Bio-Rad Laboratories, Hemel Hempstead, UK) and had been pre-filled with a cellulose suspension (a 1:1 mix of type 50 cellulose and α-cellulose, both from Sigma) in Hanks' balanced salts solution. After allowing the suspension to drain into a centrifuge tube, marrow was concentrated by centrifugation, and slides were prepared by cytocentrifuge (Shandon Cytospin 2; 1400 rpm, high acceleration for 7 min), air-dried and fixed in methanol for 10 min. The slides were stained with MGG in Sørensen buffer (pH 6.8-7.0) for 20 min at room temperature, washed twice in fresh buffer, air-dried and covered with Entellan (Merck, Germany) and cover slips. Two thousand PCEs were scored per sample for the frequency of MNPCEs and 1000 erythrocytes per sample to determine the percentages of PCEs and normochromatic erythrocytes (NCEs). Automated scoring was performed by the MetaSystems Metafer Metacyte image system (MetaSystems, Altlussheim, Germany).

Statistics: A hierarchic ANOVA, where the animal factor was hierarchical to dose factor, was used to analyse the percentage of DNA in the tail of the comets, both in BAL and lung cells. One-way ANOVA was applied to examine the frequency of positive γ-H2AX cells, both in PBMCs and lung cells. 'A posteriori' comparison among the means of doses was done by Tukey's test. The unpaired two-sample *t*-test was applied to determine whether the exposure to the positive control, WC-Co, induced a statistically significant difference as compared with the corresponding untreated control groups for the frequency of positive γ-H2AX cells, both in PBMCs and lung cells. Finally, the dose-response relationship for all the end-points analysed was investigated by linear regression analysis. The differences were interpreted to be significant if *P* was below 0.05. The statistical analyses were performed by Harvey WR (1987) and Statistix for Windows 2.0 programmes.

4 RESULTS

4.1 Immunotoxicology

4.1.1 *In vitro*

Transmission electron microscopy (TEM) was utilised to study, whether long needle-like MWCNTs; long tangled MWCNTs and asbestos are taken up by the primary macrophages. TEM images showed that all materials studied had intracellular localization in macrophages after a 6-h exposure (100 µg/ml; Fig. 4). All materials were observed free inside the cells, but not in vacuoles or in the nucleus of the macrophages. These results demonstrated no differences among the materials in uptake by primary macrophages.

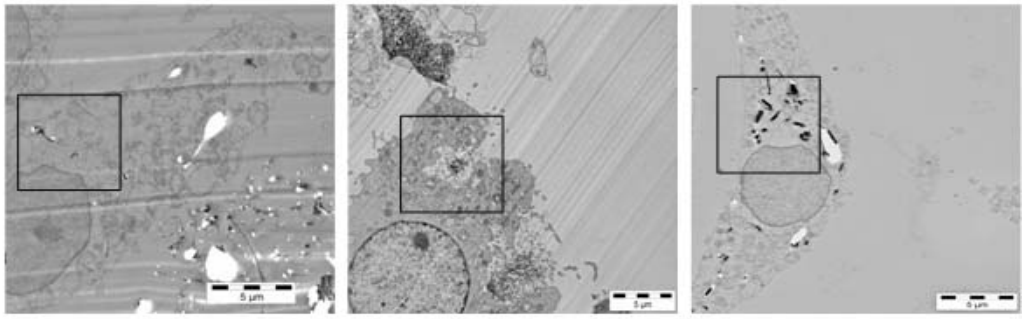

Figure 4. Transmission electron microscopic images of lipopolysaccharide-primed human primary macrophages exposed for 6 h (100 µg/ml) to long needle-like MWCNTs (left panel), long tangled MWCNTs (middle panel) and asbestos (right panel). The squares show fibers inside the cell. Measure bar is 5 µm.

Exposure of human macrophages to carbon nanomaterials or asbestos without LPS priming did not induce any IL-1α or IL-1β secretion from the macrophages (data not shown). However, IL-1α secretion was strongly induced, when LPS-primed primary macrophages were exposed to long needle-like MWCNTs (data not shown). In contrast, other types of carbon nanomaterials and asbestos were weak inducers of IL-1α secretion. The pro-IL-1β is not continuously expressed in the cytoplasm and its transcription is known to be activated after stimulation of the Toll-like receptor,

for example by bacterial LPS. However, a second signal is required for inflammasome complex formation and the cleavage of IL-1β into its active form (Martinon et al. 2002). In contrast to unprimed macrophages, LPS-primed human macrophages secreted IL-1β after exposure to carbon nanomaterials or asbestos.

In the comparison of the different materials, the long needle-like MWCNTs induced more IL-1β secretion than the other carbon nanomaterials or even asbestos (Fig. 5). Western blotting analysis confirmed that macrophages release mature IL-1β after exposure to long needle-like MWCNTs and asbestos but not after exposure to long tangled MWCNTs or short MWCNTs (Fig. 5). These data suggest that long needle-like MWCNTs are able to activate IL-1β secretion from human primary macrophages in an even more profound manner than asbestos fibers.

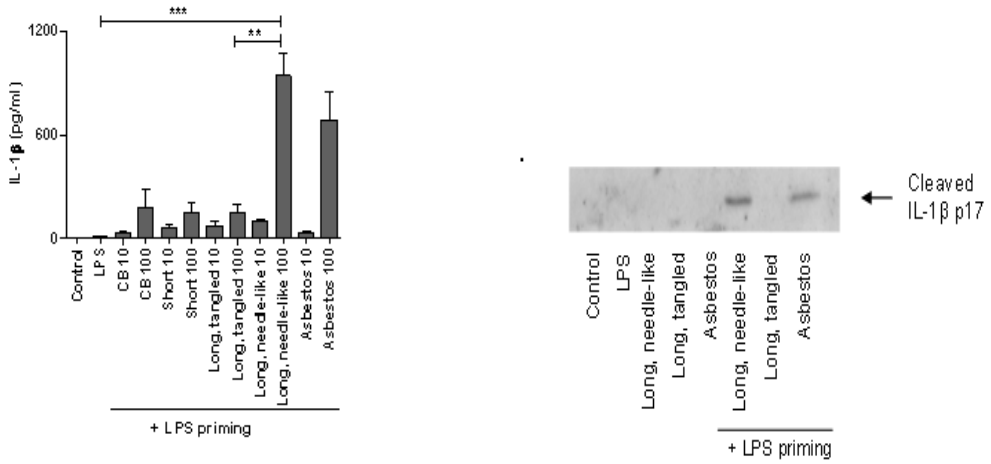

Figure 5. Long needle-like carbon nanotubes induce IL-1β secretion from lipopolysaccharide (LPS) -primed human primary macrophages. LPS-primed macrophages were exposed to carbon black, short MWCNTs; long tangled MWCNTs; long needle-like MWCNTs, and asbestos (100 µg/ml) for 6 h, cell culture supernatants were harvested and analysed for IL-1β ELISA. Secretion of cleaved IL-1β cytokine was confirmed by Western blotting analysis: The cell culture supernatants were concentrated, and IL-1β expression was analyzed by Western blotting with anti-IL-1β antibodies. All values are means ± SD from three independent analyses. **, $P < 0.01$ and ***, $P < 0.001$.

To clarify whether the NLRP3 inflammasome had been activated in response to the long needle-like MWCNTs, we performed gene silencing with NLRP3 targeting small interfering RNA in human macrophages. The NLRP3 siRNA treatment clearly decreased IL-1β secretion from macrophages after long needle-like MWCNTs and asbestos exposures (Fig. 6A, B)

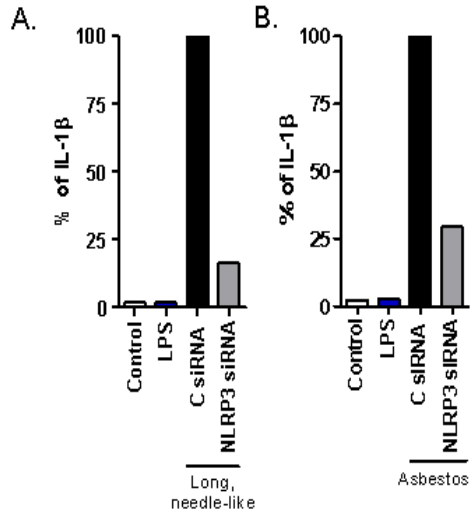

Figure 6. Needle-like multi-walled carbon nanotubes (MWCNTs) and asbestos activate NLRP3 inflammasome. Macrophages were transfected with the non-targeting siRNA control (NT-i) or the NLRP3 siRNAs (NLRP3-i) as described in materials and methods. LPS-primed human macrophages were stimulated with (A.) long needle-like MWCNTs and (B.) asbestos (100 µg/ml) for 6 h, cell culture supernatants were collected, and IL-1β ELISA was performed. The values are percentages of measured protein concentrations of two independent analyses where control siRNA = 100 %.

It is known that the extracellular ATP gating cation channel $P2X_7$ is an important upstream activator of the NLRP3 inflammasome (Kahlenberg et al., 2004, Pelegrin & Suprenant, 2006, Petrelli et al., 2007, Riteau et al., 2010). The $P2X_7$ receptor allows cations to pass through the cell membrane, e.g. K+ efflux, and this is known to be associated to the activation of the NLRP3 inflammasome (Gross et al., 2009). In an attempt to understand the role of $P2X_7$ receptor in the secretion of IL-1β evoked by long needle-like MWCNTs and asbestos, we used both pharmacological blockade and

siRNA induced inhibition of the $P2X_7$ receptor. The $P2X_7$ receptor inhibition clearly decreased IL-1β secretion from human primary macrophages (Fig. 7), suggesting that the $P2X_7$ receptor is an important molecule upstream of the NLRP3 inflammasome after exposure of cells to long needle-like MWCNTs and asbestos (Fig. 7B, C). These results demonstrate that the stimulation of the $P2X_7$ receptor is essential for the NLRP3 inflammasome activation triggered by rigid, needle-like materials.

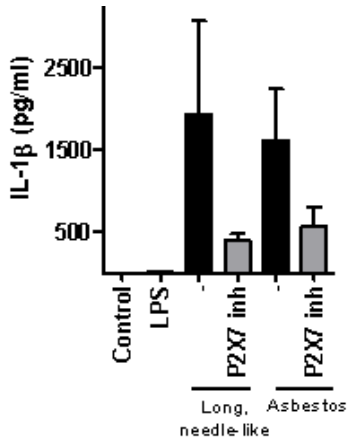

Figure 7. $P2X_7$ receptor activation is an upstream signal for NLRP3 inflammasome activation. Lipopolysaccharide (LPS) -primed human monocyte-derived macrophages were treated with long needle-like MWCNTs or asbestos (100 µg/ml) in the absence or presence of $P2X_7$ inhibitor (1 µM). Cell culture supernatants were harvested after 6 h of exposure, and IL-1β ELISA was performed.

All findings from the *in vitro* immunotoxicology studies have been published (Palomäki *et al*., 2011) and will be included in a PhD thesis.

4.1.2 *In vivo*

Acute pharyngeal aspiration exposure: A single pharyngeal aspiration exposure to long needle-like MWCNTs, long tangled MWCNTs, and asbestos all resulted in a significant influx of neutrophils into the lungs of mice (Fig. 8). Pulmonary neutrophilia is a sign of

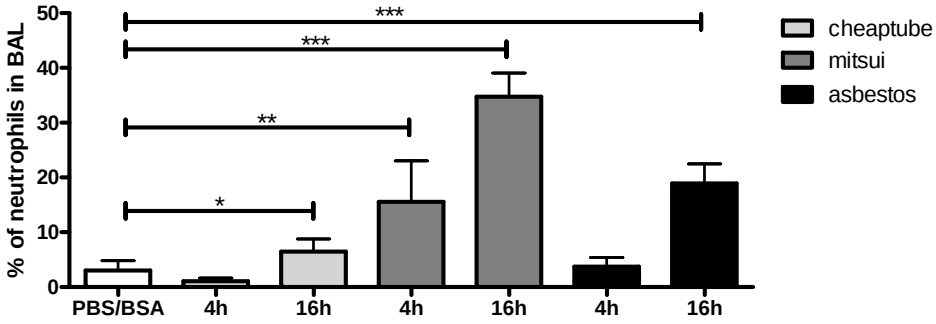

Figure 8. Percent of neutrophils of total bronchoalveolar lavage cells counted under light microscopy after exposure to PBS/BSA, long tangled MWCNTs (cheaptube), long needle-like MWCNTs (mitsui), and asbestos. The bars represent mean ± SE; *$P < 0.05$, **$P < 0.01$ and ***$P < 0.001$ significantly different from control; Mann-Whitney U test.

inflammation. Out of these three materials, long needle-like MWCNTs elicited the fastest and highest reaction reaching close to 20 % of neutrophils among BAL cells in four hours and almost 40 % in 16 h. We also looked at various inflammatory markers from the lungs of mice in the form of mRNA and proteins. Based on the results we obtained from the *in vitro* experiments, IL-1β and TNF-α were of interest. Indeed, with long needle-like MWCNTs we saw a huge increase in IL-1β 4 h after the aspiration exposure (Fig. 9). TNF-α, on the other hand, was significantly elevated only with asbestos exposure (Fig. 9).

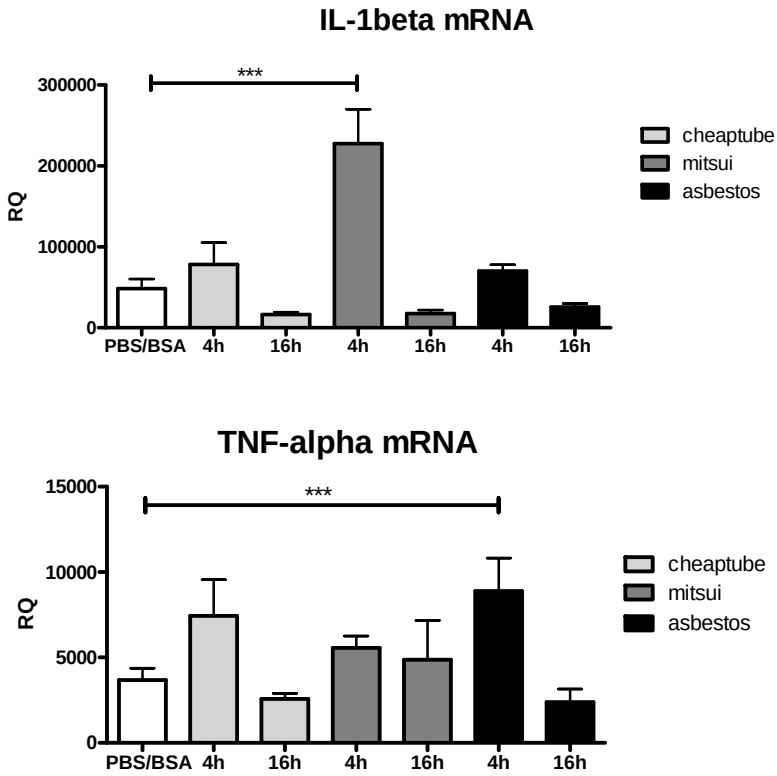

Figure 9. mRNA-expression in lung tissue by proinflammatory cytokines *IL-1β* and *TNF-α*. Results are shown as relative quantity (RQ) for mice exposed to PBS/BSA, long tangled MWCNTs (cheaptube), long needle-like MWCNTs (mitsui) and asbestos and sacrificed 4 and 16 h after the exposure. All values are presented as means ± SD. *** $P < 0.001$, significantly different from control; Mann-Whitney U test.

Another interesting finding was the elevation of *CXCL5*, a neutrophil-attracting chemokine (Fig. 10). After four hours of exposure to long needle-like MWCNTs, we observed a huge increase in *CXCL5* expression. Also with asbestos the levels were significantly increased. This correlated with pulmonary neutrophilia seen with both long needle-like MWCNTs and asbestos exposure (Fig. 10).

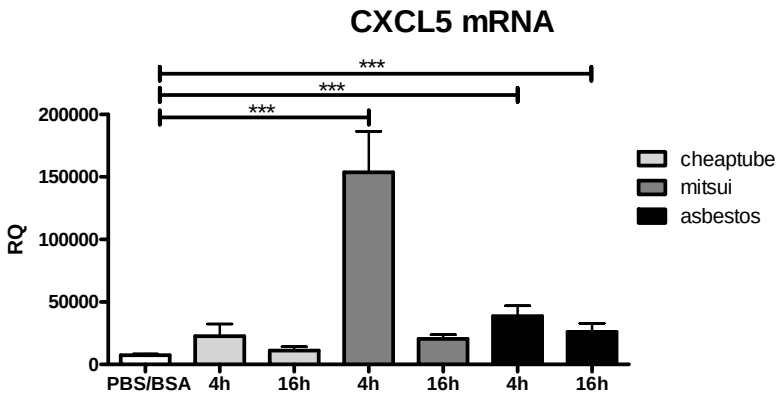

Figure 10. mRNA-expression in the lung tissue of neutrophil attracting chemokine *CXCL5*. Results are shown as relative quantity (RQ) for PBS/BSA, long tangled MWCNTs (cheaptube), long needle-like MWCNTs (mitsui), and asbestos exposed mice sacrificed 4 and 16 h after the exposure. All values are presented as means ± SD where ***$P <$ 0.001 001 significantly different from control; Mann-Whitney U test.

On protein level, we found interesting results with CXCL9, CXCL1 and CCL3. CXCL9 was increased significantly after exposure to long needle-like MWCNTs but not with long tangled MWCNTs or asbestos (Fig. 11). CXCL9 is a T-cell chemoattractant which is known

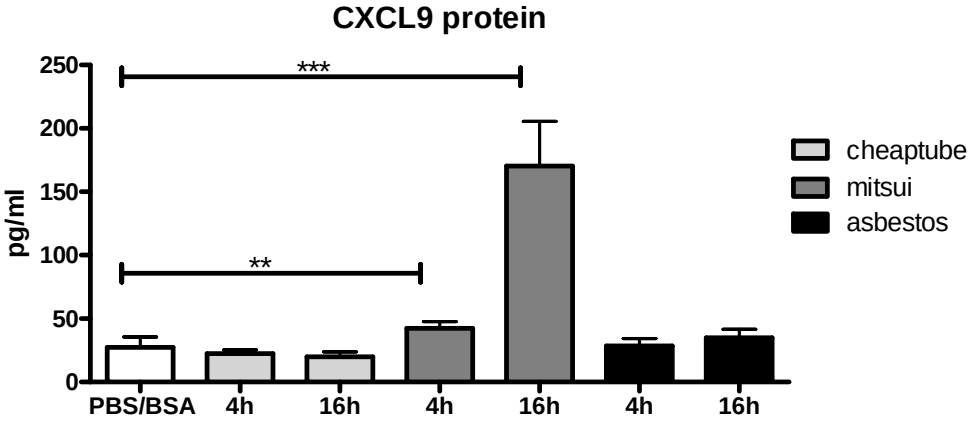

Figure 11. Protein expression of T-cell chemoattractant CXCL9 in bronchoalveolar lavage. Results are shown as relative quantity (RQ) for PBS/BSA, long tangled MWCNTs (cheaptube), long needle-like MWCNTs (mitsui), and asbestos exposed mice sacrificed 4 and 16 h after the exposure. All values are presented as means ± SD where **$P <$ 0.01 and ***$P <$ 0.001, significantly different from control; Mann-Whitney U test.

to be induced by IFN-γ. This correlated with increased amount of lymphocytes seen only in mice exposed to long needle-like MWCNTs (data not shown).

CXCL1 is expressed by macrophages, neutrophils and epithelial cells and has neutrophil chemoattractant activity. Accordingly, it was seen at high levels after four hours after all exposures (Fig. 12). At 16 h, CXCL1 was still elevated for long needle-like MWCNTs. Neutrophilia seems to be a common reaction to particles which can be seen with all materials, its degree reflecting the harmfulness of the material.

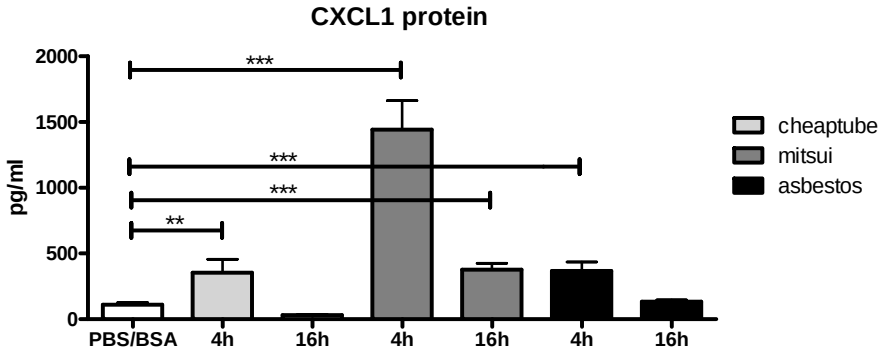

Figure 12. Protein expression of CXCL1, a neutrophil chemoattractant, in broncho-alveolar lavage. Results are shown as pg/ml for PBS/BSA, long tangled MWCNTs (cheaptube), long needle-like MWCNTs (mitsui), and asbestos exposed mice sacrificed 4 and 16 h after the exposure. All values are presented as means ± SD. $^{**}P < 0.01$ and $^{***}P < 0.001$, significantly different from control; Mann-Whitney U test.

Another protein that was expressed considerably more with long needle-like MWCNTs than the other materials was CCL3 (Fig. 13). CCL3 is known as macrophage inflammatory protein-1α (MIP-1α) and it is a cytokine that is involved in the acute inflammatory state in the recruitment and activation of polymorphonuclear leukocytes i.e. neutrophils and eosinophils.

Chronic pharyngeal aspiration exposure: A single pharyngeal aspiration exposure to long needle-like MWCNTs with sampling after 28 days resulted in pulmonary granulomas filled with CNTs and mucus-producing goblet cells (Fig. 14).

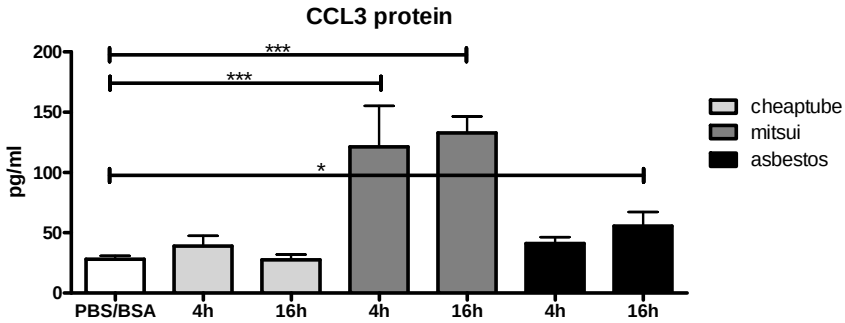

Figure 13. Protein expression of CCL3, an acute inflammatory protein, in bronchoalveolar lavage. Results are shown in relative pg/ml for PBS/BSA, long tangled MWCNTs (cheaptube), long needle-like MWCNTs (mitsui), and asbestos exposed mice sacrificed 4 and 16 h after the exposure. All values are presented as means ± SD. $^{**}P < 0.01$ and $^{***}P < 0.001$, significantly different from control; Mann-Whitney U test.

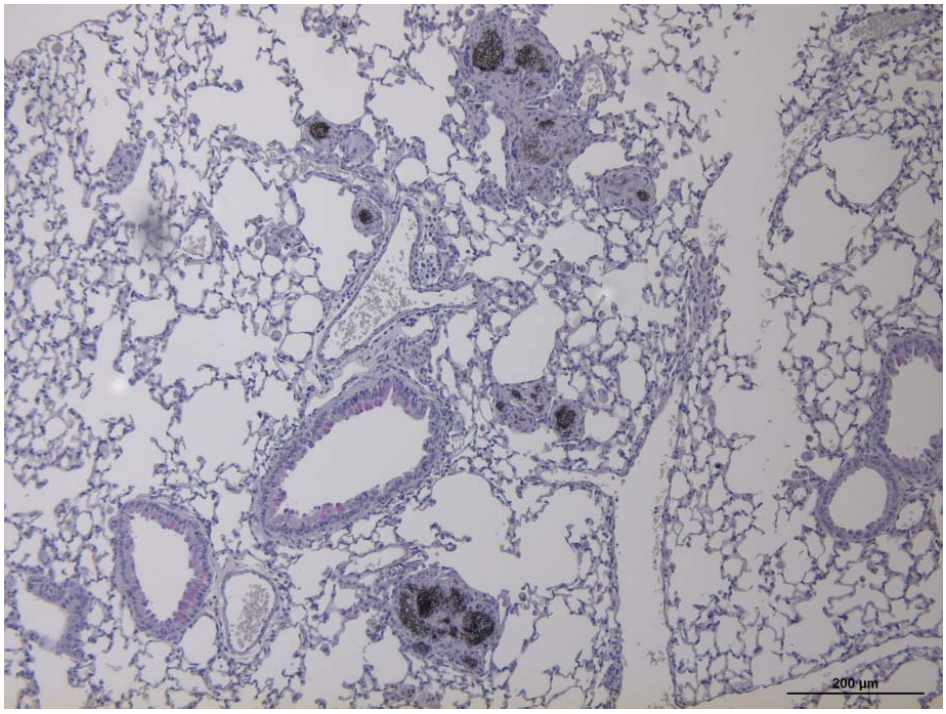

Figure 14. Periodic acid-Schiff (PAS) -stained mouse lung tissue, where mucus-producing goblet cells can be seen in red colour around the bronchioles. Black clumps of long needle-like multiwall carbon nanotubes are inside and surrounded by granulomas.

Inhibition using antagonists: To find out whether TNF-alpha and IL-1β indeed had a significant part in the inflammation process, we used etanercept and anakinra to block TNF-alpha and IL-1β, respectively.

Etanercept and Anakinra are drugs developed to treat autoimmune diseases and rheumatoid arthritis, respectively. Etanercept acts as a TNF inhibitor by binding to TNF-alpha. Anakinra blocks the biological activity of IL-1 by competitively inhibiting the binding of IL-1 to the interleukin-1 type receptor.

Both antagonists given separately and together resulted in a significant decrease in neutrophilia (Fig. 15) and mRNAs of *IL-1β* and *TNF-α* (Fig. 16) which were expressed after the single pharyngeal aspiration exposure to long needle-like MWCNTs.

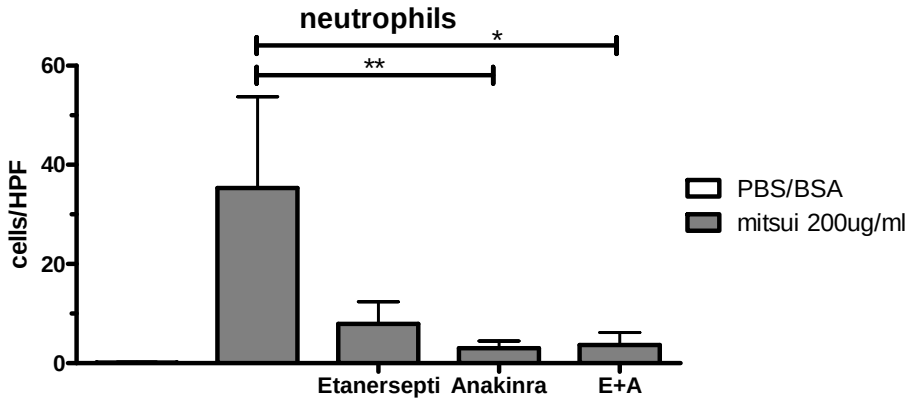

Figure 15. The effect of a single pharyngeal aspiration exposure on neutrophil infiltration to bronchoalveolar lavage fluid calculated from May–Grünwald–Giemsa (MGG)-stained cytospin slides with light microscopy (x40). Results are shown as cells per high power field (HPF) for PBS/BSA and long needle-like multi-walled carbon nanotubes (mitsui) exposed mice treated with antagonists of TNF-α (etanersepti), IL-1β (anakinra) or both (E+A). The bars represent mean ± SE; * $P < 0.05$ and ** $P < 0.01$, significantly different from control; Mann-Whitney U test.

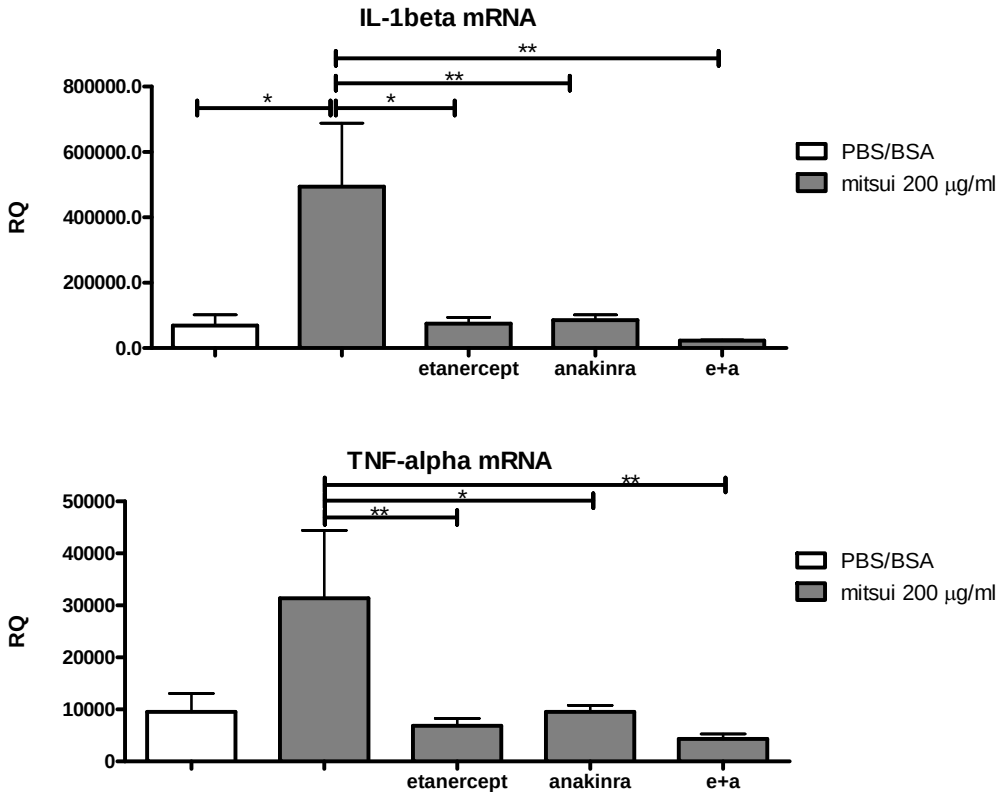

Figure 16. mRNA-expression in the lung tissue of proinflammatory cytokines *IL-1β* and *TNF-a*. Results are shown in relative quantity (RQ) for mice exposed to PBS/BSA and long needle-like multiwall carbon (mitsui) and treated with antagonists of TNF-alpha (etanersepti), IL-1β (anakinra) or both (e+a). All values are presented as means ± SE. ***$P < 0.001$ significantly different from control; Mann-Whitney U test.

Acute inhalation exposure to long needle-like multi-walled carbon nanotubes: Inhalation exposure to long needle-like MWCNTs resulted in a significant increase in inflammatory cells, i.e. neutrophils, eosinophils and lymphocytes, in the BAL of the mice (Fig. 17). Neutrophils are usually the first cells to respond to inflammation and they migrate to the site in the acute phase. They are the hallmark of acute inflammation and an essential part of the innate immune system. Eosinophils and lymphocytes, on the other hand, are usually associated with allergic or atopic diseases and the adaptive immune response.

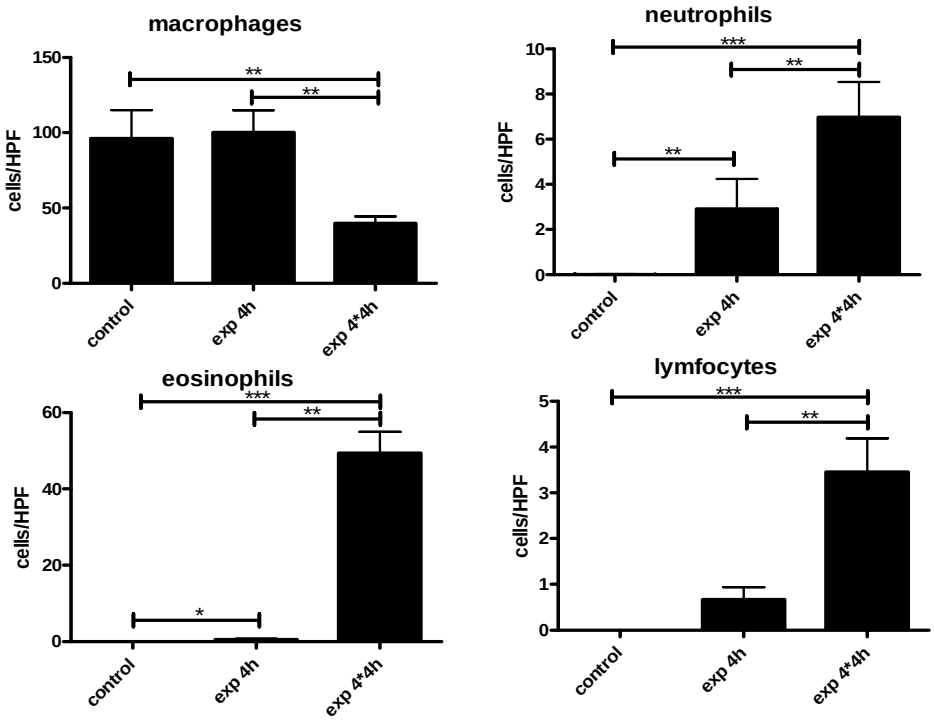

Figure 17. Effect of inhalation exposure to long needle-like multi-walled carbon nanotubes (MWCNTs; mitsui) on infiltration of macrophages, neutrophils, eosinophils, and lymphocytes to bronchoalveolar lavage fluid calculated from May–Grünwald–Giemsa (MGG)-stained cytospin slides with light microscopy (x40). Results are shown as cells per high power field (HPF) for control mice and mice exposed to long needle-like MWCNTs for 4 h or 4 h on four consecutive days. The bars represent mean ± SE; * $P < 0.05$, ** $P < 0.01$ and ***$P < 0.001$, significantly different from unexposed control; Mann-Whitney U test.

In addition to a flood of inflammatory cells in the BAL, we also encountered some foreign-body giant cells (Fig. 18). They are collections of fused macrophages. These cells are generated in response to large foreign bodies and are particularly common with particles that cause chronic inflammation and the foreign body response.

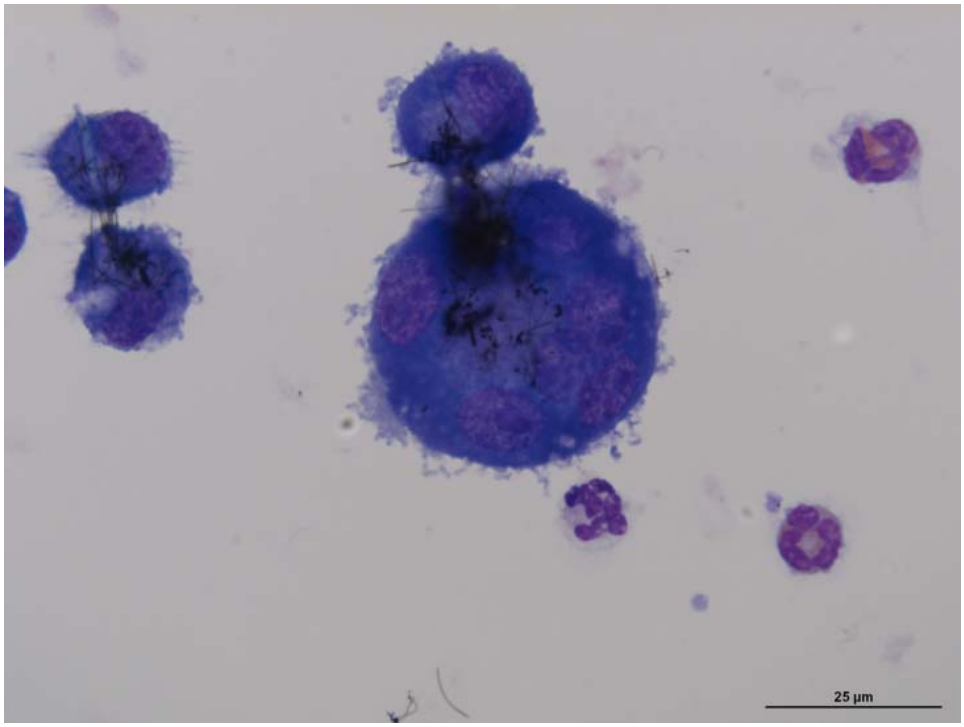

Figure 18. May–Grünwald–Giemsa-stained cytospin slide under light microscopy showing a neutrophil and eosinophils together with long needle-like multiwall carbon nanotubes between a macrophage and a foreign-body giant cell. Bar 25 µm.

IL-1β was significantly expressed on protein level after inhalation of long needle-like MWCNTs (Fig. 19). On mRNA level, *IL-13* and *CCL17* were significantly upregulated (Fig. 19). IL-13 is involved with allergic lung diseases and is an important factor in inducing airway hyperresponsiveness, goblet cell metaplasia and mucus hypersecretion. In addition, it also induces secretion of chemokines that recruit allergic effector cells to the lungs. CCL17 specifically binds and induces chemotaxis in T cells.

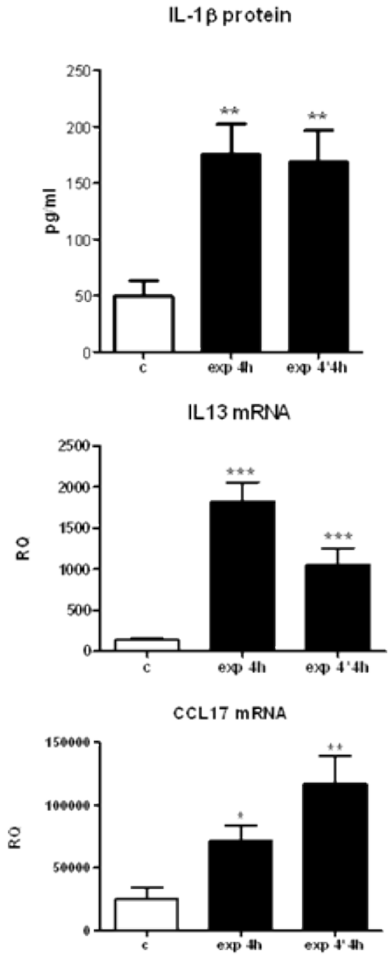

Figure 19. Expression of proinflammatory protein IL-1β in bronchoalveolar lavage and lung tissue mRNA expression of IL-13 and CCL17. Results are shown in pg/ml and relative quantity (RQ) for control mice and mice exposed to long needle-like multi-walled carbon nanotubes for 4 h or for 4 h on four consecutive days. The bars represent mean ± SE; * *P* 0.05, ** *P* 0.01 and ****P* < 0.001, significantly different from unexposed control; Mann-Whitney U test.

4.2 Genotoxicology

4.2.1 *In vitro*

Cytotoxicity: Long needle-like MWCNTs (Mitsui-7) induced a clear dose-dependent decrease in the number of BEAS 2B cells after all treatment times (4 h, 24 h and 48 h), as measured by the Trypan blue assay (Fig. 20A,). Cytotoxicity exceeding 50 % occurred approximately at 200 µg/cm^2 for all time points. The luminescent cell viability assay (measuring ATP) showed similar results, although >50% cytotoxicity occurred already at about 80 µg/cm^2 at each time point (Fig. 20B).

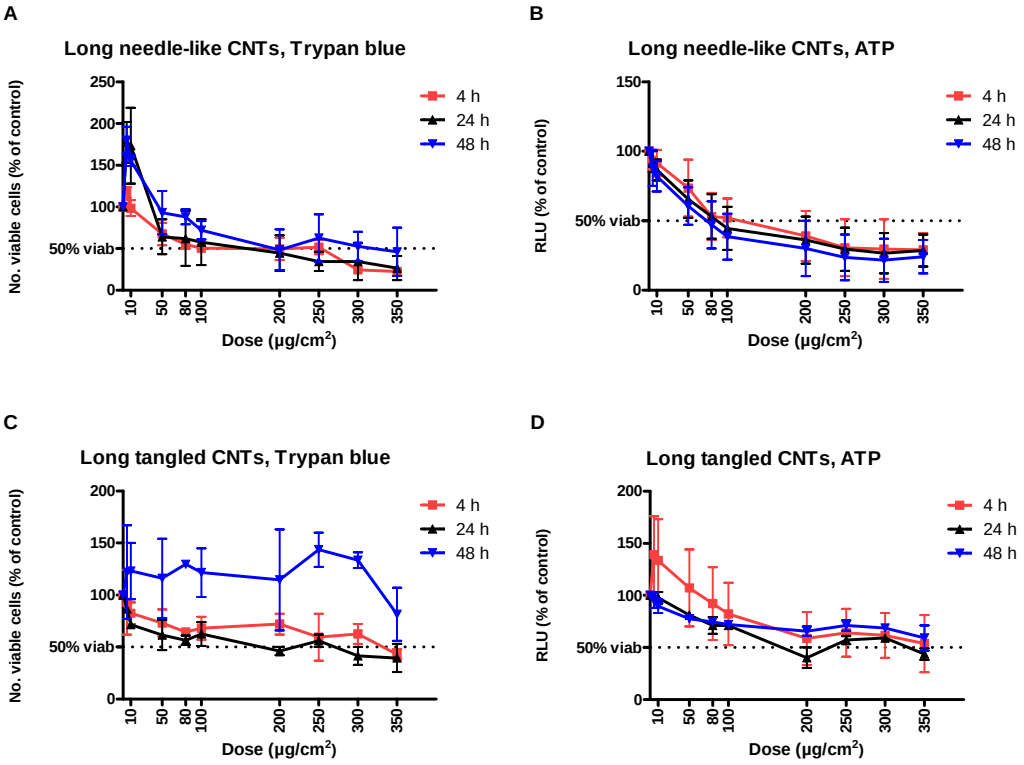

Figure 20. The number of viable cells (control = 100 %; Trypan blue exclusion) or ATP level (luminescent cell viability assay; RLU, relative luminescence units) after treatment with the multi-walled carbon nanotubes studied. The 50 % limit of viable cell number is marked with a dotted line.

Long tangled MWCNTs (Cheaptubes) induced a slight dose-dependent decrease in the number of living cells after the 4-h and 24-h treatments, but not after the 48-h treatment (Fig. 20C). Over 50 % cytotoxicity was seen at 350 μg/cm^2 after the 4-h treatment and at 200 μg/cm^2 after the 24-h treatment. Similar results were seen in the ATP assay, except that also the 48-h treatment showed a dose-dependent cytotoxic effect (Fig. 20D).

DNA damage: Long needle-like MWCNTs significantly ($P < 0.01$) increased the level of DNA damage, as measured by the comet assay, at most doses tested, already the lowest dose (5 μg/cm^2) showing a 2.1-fold increase in comparison with the control (Fig. 21). Although the level of DNA damage did not further increase after 10 μg/cm^2, there was a borderline dose-dependent effect ($P = 0.06$; Fig. 21).

Long tangled MWCNTs induced a lower level of DNA damage, with only the highest dose (250 μg/cm^2) significantly ($P < 0.05$; 1.6-fold increase) differing from the control (Fig. 21); yet, the increase was dose-dependent ($P < 0.001$). Again, after an initial small increase in DNA damage (not significant) at low doses there was very little further elevation at higher doses. The positive dose of long tangled MWCNTs (250 μg/cm^2) showed rather high cytotoxicity after the 24 h treatment, indicating near 50 % cytotoxicity (in comparison with the controls) by both the Trypan blue and the luminometric assays (Fig. 20C, D).

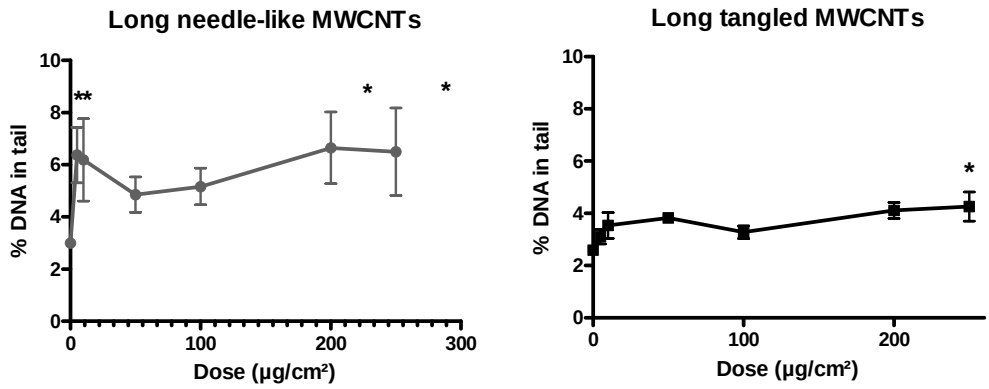

Figure 21. Induction of DNA damage (comet assay) in human bronchial epithelial BEAS 2B cells by a 24-h treatment with long needle-like and long tangled multi-walled carbon nanotubes (MWCNTs). DNA damage is expressed as percentage of DNA in comet tail (%DNA in tail). Symbols represent means, error bars SEM between duplicate cultures. *, statistically significantly different from the controls.

Micronuclei and CBPI: Neither long needle-like MWCNTs nor long tangled MWCNTs were able to induce micronuclei in BEAS 2B cells (Fig. 22). However, there was a significant negative dose-response for the long needle-like MWCNTs ($P < 0.01$) and a similar trend for the long tangled MWCNTs. The nanomaterials covered the slides at the highest concentrations and made the analysis impossible for 40 µg/cm^2 and higher doses of long needle-like MWCNTs and for doses over 200 µg/cm^2 of long tangled MWCNTs. CBPI decreased dose-dependently ($P < 0.01$) following exposure to both of the MWCNTs (Fig. 22), indicating an induction of cell cycle delay.

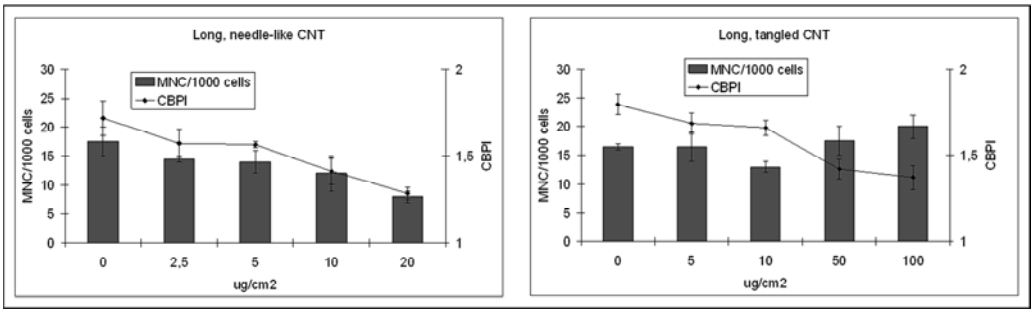

Figure 22. Cytokinesis-block micronucleus assay with long needle-like and long tangled multi-walled carbon nanotubes (MWCNTs) in BEAS 2B cells. 1000 binucleate cells scored per culture (2000 per experimental point) for the No. of micronucleated binucleate cells (MNC; columns) and 200 cells (400 per experimental point) for cytokinesis-block proliferation index (CBPI; symbols). Columns and symbols represent means, error bars SEM between duplicate cultures.

4.2.2 *In vivo*

Pharyngeal aspiration. Fig. 23 shows the results of the Comet assay on BAL cells and lung cells 24 h after pharyngeal aspiration exposure to long needle-like and long tangled MWCNTs. A significant, 3.5-fold increase ($P = 0.002$) in the percentage of DNA in tail in the lung cells, compared with vehicle-treated animals, was found at the highest dose (200 µg) of long needle-like MWCNTs, with a very clear positive dose-response ($P < 0.0001$). Long tangled MWCNTs caused no significant increase in DNA damage in BAL or lung cells - in fact there was a significant negative dose-response ($P < 0.05$) in both cell types. The positive control, WC-Co (1 mg/mouse), increased the percentage of DNA in tail (in comparison with the controls) by 1.5-1.8-fold in the lungs and 1.7-2.8-fold in BAL cells.

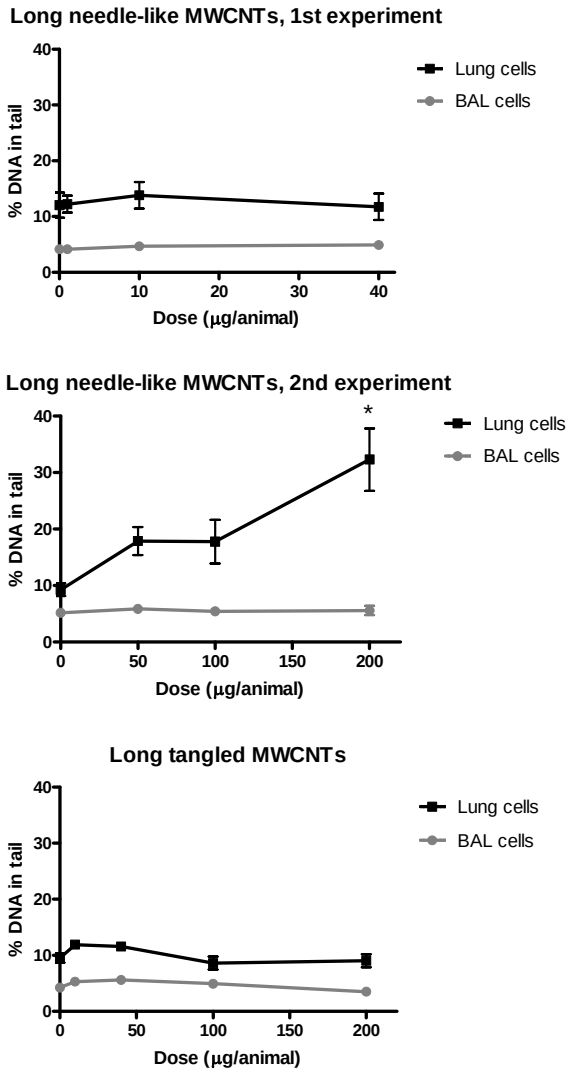

Figure 23. Induction of DNA damage (comet assay) in bronchoalveolar lavage (BAL) cells and lung cells 24 h after pharyngeal aspiration of long needle-like and long tangled multi-walled carbon nanotubes (MWCNTs). Note that the 1st experiment (upper panel) included a lower dose range (10-40 µg/animal) than the other experiments (middle and lower panels; 50-200 µg/animal). Symbols represent means of 6 animals per group, error bars are SEM. The asterisk indicates a significant effect (as compared with the control group) of long needle-like MWCNTs on DNA damage in lung cells; there was also a significant positive dose-response (linear regression analysis; $P < 0.0001$). The positive control, tungsten carbide-cobalt mixture produced a 1.5-1.8-fold (lung cells) and a 1.7-2.8-fold (BAL) increase in % DNA in tail in comparison with the controls.

The frequencies of γ-H2AX positive cells, indicative of DNA double-strand break repair, among PBMCs and lung cells obtained from the pharyngeal aspiration experiment are shown in Table 3. Long needle-like MWCNTs did not significantly increase the frequency of γ-H2AX positive cells at any of the tested doses (1-200 μg/mouse) in peripheral blood or in lungs. No significant linear dose-response relationship could be found in the first experiment where lower doses (1-40 μg/mouse) were applied. However, a linear dose-response of borderline significance (P = 0.059) was seen in lung cells but not in PBMNs in the second experiment where higher doses were tested (50-200 μg/mouse). Long tangled MWCNTs showed no significant increase in the level of DNA damage at any of the tested doses (1-200 μg/mouse) in either tissue. No significant linear dose response could either be found in PBMNs. In lung cells, a significant negative dose response (P = 0.021) was seen. WC-Co, used as a positive control for the comet assay in BAL and lung cells, did not significantly increase the frequency of γ-H2AX positive cells in lung cells or PBMCs. In general, the baseline level of γ-H2AX positive cells was 6-8 times higher in PBMCs than in lung cells (Table 3).

Inhalation exposure. Results from the inhalation exposure to long needle-like MWCNTs (~8 mg/m^3 for 4 days, 4 h/day) are shown in Figs 24-26. DNA damage, as measured by the percentage of DNA in comet tail (Fig. 24) was significantly increased ($P < 0.05$) by the MWCNT exposure, both in BAL and lung cells. DNA damage was induced particularly in BAL cells where a 6-fold higher was seen in comparison with the control group. The positive control treatment, WC-Co (1 mg/mouse), induced 1.2-fold and 2.1-fold increases in the percentage of DNA in tail in lung cells and BAL cells, respectively.

Long needle-like MWCNTs did not induce systemic genotoxic effects in blood leukocytes, as measured by the presence of γ-H2AX foci (Fig. 25), or in bone marrow, as determined by the micronucleus assay (Fig. 26). The positive control Mitomycin C (2 mg/kg intraperitoneally) was clearly positive in both assays.

Table 3. Frequencies of γ-H2AX positive cells among peripheral blood mononuclear leukocytes and lung cells of mice 24 h after pharyngeal aspiration to long needle-like and long tangled multi-walled carbon nanotubes (MWCNTs).

Exposure dose (µg/animal)	**Long needle-like MWCNTs**						**Long tangled MWCNTs**		
	Experiment 1 (low doses)			Experiment 2 (high doses)					
	No. animals[a]	Mean (SD) No. γ-H2AX positive cells among 1000 lung cells	Mean (SD) No. γ-H2AX positive cells among 1000 blood leukocytes	No. animals[a]	Mean (SD) No. γ-H2AX positive cells among 1000 lung cells[b]	Mean (SD) No. γ-H2AX positive cells among 1000 blood leukocytes	No. animals[a]	Mean (SD) No. γ-H2AX positive cells among 1000 lung cells[c]	Mean (SD) No.γ-H2AX positive cells among 1000 blood leukocytes
0	5	2.5 (0.6)	15.4 (6.3)	6	4.5 (3.7)	28.0 (8.3)	6	3.0 (2.2)	24.2 (16.1)
1	4	3.0 (3.2)	23.0 (16.3)						
10	5	4.6 (1.5)	22.6 (25.6)				6	6.5 (4.1)	27.8 (21.6)
40	5	4.2 (4.6)	15.6 (7.2)				6	4.3 (2.4)	13.3 (3.3)
50				6	3.3 (1.7)	21.3 (16.4)			
100				6	5.6 (3.3)	22.3 (10.4)	6	0.8 (0.7)	20.3 (9.4)
200				6	6.8 (2.2)	16.5 (8.4)	5	1.6 (2.6)	17.0 (7.0)
WC-Co (1 mg/animal)	3	7.3 (4.2)	16.0 (6.2)	6	2.3 (1.7)	18.2 (6.8)	4	1.5 (1.3)	19.0 (13.9)

[a] 1000 cells were scored per animal and tissue.
[b] Borderline significant positive dose response ($P = 0.059$), linear regression analysis.
[c] Significant negative dose response ($P = 0.021$), linear regression analysis.

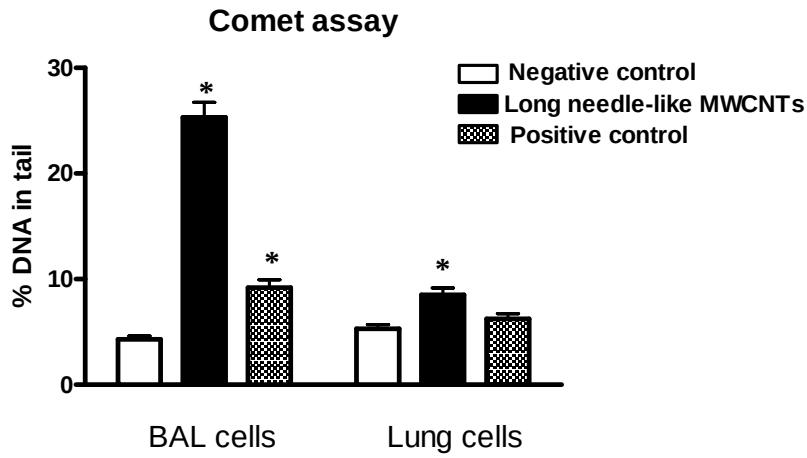

Figure 24. Mean (+SEM) percentage of DNA in tail (comet assay) in bronchoalveolar lavage (BAL) cells and lung cells of mice exposed to long needle-like multi-walled carbon nanotubes (MWCNTs) by inhalation (~8 mg/m^3 for 4 days, 4 h/day) or to tungsten carbide-cobalt mixture (pharyngeal aspiration, 1 mg/mouse; positive control). Asterisks indicate a significant difference ($P < 0.05$) in comparison with the negative control group.

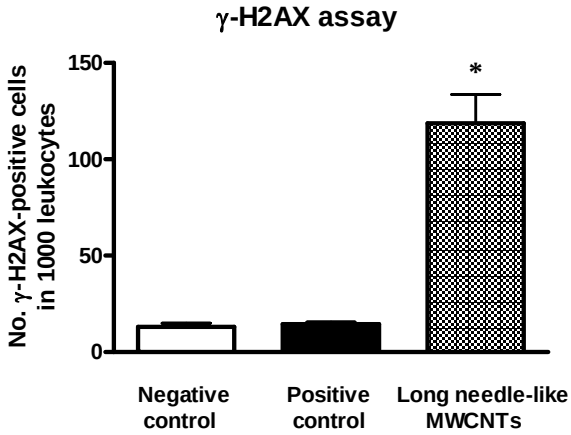

Figure 25. Frequency of γ-H2AX-positive cells in 1000 peripheral blood mononuclear leukocytes of mice (2000 cells scored per animal) exposed to long needle-like multi-walled carbon nanotubes (MWCNTs) by inhalation (~8 mg/m^3 for 4 days, 4 h/day) or to mitomycin C (2 mg/kg i.p.; positive control; sampling 24 h after treatment). Columns represent means, error bars SEM. Asterisks indicate a significant difference ($P < 0.05$) in comparison with the negative control group.

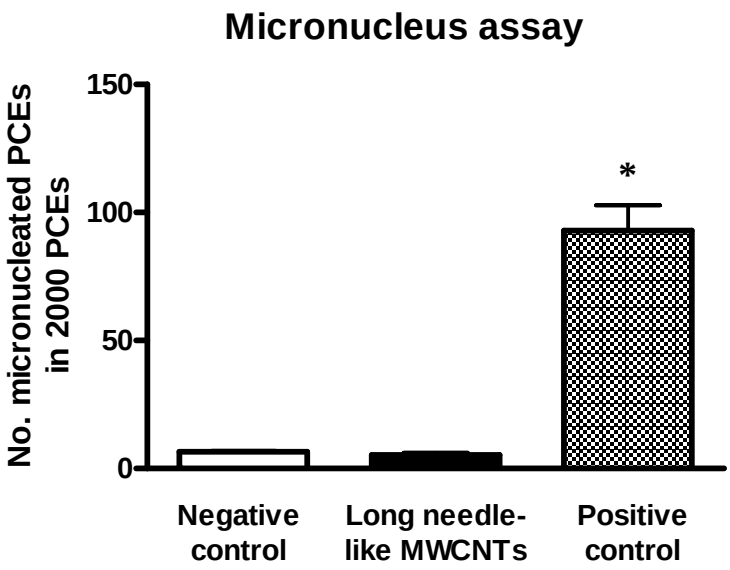

Figure 26. Frequency of micronucleated polychromatic erythrocytes (PCEs) among 2000 PCEs in bone marrow of mice exposed to long needle-like multi-walled carbon nanotubes (MWCNTs) by inhalation (~ 8 mg/m^3 for 4 days, 4 h/day) or to mitomycin C (2 mg/kg i.p.; positive control; sampling 24 h after treatment). Columns represent means, error bars SEM. Asterisks indicate a significant difference ($P < 0.05$) in comparison with the negative control group.

5 CONCLUSIONS AND DISCUSSION

Long needle-like MWCNTs induced inflammation in both cultured cells and mice. In the lungs, we saw a clear increase in inflammatory cells and proinflammatory cytokines and chemokines. The inflammatory response was stronger with long needle-like carbon nanotubes than with crocidolite asbestos. The cytokine IL-1β and the inflammasome complex appeared to be in a central position in the mechanism leading to inflammation. Neutrophils were the key effector cells in mice exposed by aspiration and eosinophils in mice exposed by inhalation.

The inflammation produced by inhaled long needle-like MWCNTs greatly resembled allergic asthma, which is most exceptional. Such a reaction caused by particle exposure alone is unseen in mice without sensitisation. Especially the induction of IL-13 and eosinophils was surprising.

In vivo, the features and severity of the inflammation depended on the type of exposure. Long needle-like MWCNTs invoked a much stronger inflammation when administered by inhalation as an aerosol than by pharyngeal aspiration as dispersion. This may have been due to proteins covering the dispersed particles, while inhaled particles reached the lungs bare and without a protein corona. Protein corona may dampen the particle-cell reactions by changing the appearance of MWCNTs as seen by the cells. Another factor possibly influencing the differential response is the dose rate. In pharyngeal aspiration, MWCNTs were delivered as a single bolus, whereas more gradual exposure, 4 h/day for 4 days, was applied in the inhalation experiment.

Both long needle-like and long tangled MWCNTs induced a dose-dependent increase in DNA damage in cultured human bronchial epithelial BEAS 2B cells. While long-needle-like MWCNTs significantly increased the level of DNA damage already at the lowest dose tested, long tangled MWCNTs produced a significant increase in DNA damage only at a 50-fold higher, cytotoxic dose. Therefore, the effect of long tangled MWCNTs could only be considered borderline positive. Neither of the MWCNTs was able to induce chromosome damage *in vitro*, as judged by the micronucleus assay.

In vivo in mice, long needle-like MWCNTs were able to increase DNA damage in lung cells after exposure by inhalation and pharyngeal aspiration. It was remarkable that the DNA-damaging effect of long needle-like MWCNTs was clearer *in vivo* than *in vitro*. The weak

DNA-damaging potential of long tangled MWCNTs seen at the highest dose *in vitro* could not be reproduced *in vivo*. These findings suggest limited predictivity for the *in vitro* DNA damage assay with respect to the production of *in vivo* DNA damage. It is, however, unclear if the mechanisms of DNA damage induction by long, needle-like MWCNTs were entirely the same *in vitro* and *in vivo*. Although oxidative stress may have played a role in DNA damage induction by MWCNTs in both conditions, secondary genotoxic effects associated with inflammation - which cannot fully be produced *in vitro* - may have been important *in vivo*.

Exposure to long needle-like MWCNTs produced an increase in lung cell DNA damage concurrently with the pulmonary influx of inflammatory cells and activation of various proinflammatory cytokines and chemokines. At this stage, it is still too early to tell if these two phenomena just occurred at the same time or if the genotoxic effect actually was secondary to inflammation. If the DNA damage was associated with reactive oxygen species produced by inflammatory cells such as neutrophils, a rather strong increase in these cells was needed, because the slight pulmonary neutrophilia brought about by pharyngeal aspiration of long tangled MWCNTs did not result in DNA damage.

In BAL cells, long needle-like MWCNTs induced a high increase in DNA damage after inhalation exposure but had no effect after pharyngeal aspiration. This may suggest that macrophages, which constitute the majority of BAL cells, are more sensitive to the genotoxicity of long needle-like MWCNTs after exposure by inhalation than pharyngeal aspiration. The pharyngeal aspiration used delivered a high dose at a single administration of MWCNT dispersion, while the total dose was lower and dose rate much slower in the 4-day, 4 h/day inhalation exposure to MWCNT aerosol. It is presently unclear how these differences could explain the results. The high acute exposure by the pharyngeal aspiration may have resulted in a quick overload of macrophages with particles followed by their replacement with fresh cells less exposed to MWCNTs. Alternatively, the pulmonary eosinophilia induced by the inhalation but not by the pharyngeal exposure may have contributed by a secondary genotoxic effect. It is also possible that albumin, used in dispersing MWCNTs in the pharyngeal aspiration study, affected macrophage reaction towards MWCNTs.

Long needle-like MWCNTs did not induce MN in bone marrow of mice after inhalation exposure. This finding agreed with the negative results obtained with the MN assay *in*

vitro. MWCNTs neither produced γ-H2AX foci, indicative of DNA double strand breaks, in mouse lung cells or PBMNs. These results suggest that long needle-like MWCNTs do not have local or systemic clastogenic (chromosome-breaking) or aneugenic effects under the exposure conditions studied.

In conclusion, our study underlined the special toxicity of long and needle-like MWCNTs, revealing completely new effects such as asthma-like inflammation and DNA damage in the lungs. Our findings suggest that the rigidity of long carbon nanotubes is a central characteristic with respect to their harmful effects. Long needle-like MWCNTs, more than 50 nm thick, produced a strong inflammation and were genotoxic, while thinner (8-15 nm) and flexible tangled MWCNTs, which tend to form agglomerates, had hardly any effects. Further mechanistic understanding of the inflammatory and genotoxic effects of MWCNTs is urgently needed. Therefore, we have continued our investigations deeper into the mechanisms of the exceptional inflammatory response observed and into the possible connections between inflammation and genotoxic effects. We are interested in finding out (a) what cell types are involved in launching the extraordinary inflammatory reaction, (b) why especially long and needle-like carbon nanotubes are particularly toxic, and (c) if oxidative stress and inflammation could explain, and by which mechanism, the concurrent genotoxic effects.

Our findings provide new information on the adverse effects of MWCNTs and are useful in assessing which forms of MWCNTs require regulatory attention and special safety measures in occupational settings.

6 DISSEMINATION OF KNOWLEDGE

Besides the present report, our results will be published in international and domestic scientific literature. One such publication has already appeared (Palomäki *et al.*, 2011) and others are in preparation. The findings will also be presented in international and domestic scientific conferences, symposia and workshops, in committees dealing with the safety of nanomaterials, and within the Nanosafety Cluster of the European Commission. The research carried out in this project will form a part of two doctoral theses which are in preparation.

During this project, we improved our practices in work with nanomaterials, including a complete renewal of the exposure facilities and safety precautions. We determined the special requirements that handling of nanomaterials sets for the working space, ventilation, and personal protection. Comprehensive alterations were introduced to ascertain safety. Detailed instructions for safe work with nanomaterials were prepared and communicated to the staff. The outcome of this process was utilized in defining a model solution applicable to this type of MWCNT exposure. Action plans for dealing with occupational exposure to nanomaterials are further being developed in another project (Finnish Work Environment Fund, No. 112132).

The mechanisms behind the immunotoxic effects of MWCNTs described in this report were further characterized in a subsequent project supported by the Finnish Work Environment Fund (No. 110168; see Sund *et al*., 2013). Another project, concentrating on the genotoxic mechanisms of nanomaterials (including MWCNTs), is presently in progress (Finnish Work Environment Fund, No. 112248).

7 REFERENCES

Adlakha-Hutcheon, G., Khaydarov, R., Korenstein, R., Varma, R., Vaseashta, A., Stamm, H., *et al*. Nanomaterials, nanotechnology: applications, consumer products, and benefits. In: Linkov, I., Steevens, J., (eds), *Nanomaterials: risks and benefits*. Dordrecht: Springer, 2009, p. 195–207.

Bonassi, S.; Norppa, H.; Ceppi, M.; Strömberg, U.; Vermeulen, R.; Znaor, A.; Cebulska-Wasilewska, A.; Fabianova, E.; Fucic, A.; Gundy, S.; Hansteen, I.-L.; Knudsen, L.E.; Lazutka, J.; Rossner, P.; Sram, R.J.; Boffetta, P. Chromosomal aberration frequency in lymphocytes predicts the risk of cancer: results from a pooled cohort study of 22.358 subjects in 11 countries. *Carcinogenesis* 2008, 29:1178-1183.

Catalán, J., Järventaus, H., Vippola, M., Savolainen, K., Norppa, H. Induction of chromosomal aberrations by carbon nanotubes and titanium dioxide nanoparticles in human lymphocytes in vitro. *Nanotoxicology* 2012, 6:825-836.

Cortez, B.A., Machado-Santelli, G.M. Chrysotile effects on human lung cell carcinoma in culture: 3-D reconstruction and DNA quantification by image analysis. *BMC Cancer* 2008, 8:181.

De Volder, M.F., Tawfick, S.H., Baughman, R.H., Hart, A.J. Carbon nanotubes: present and future commercial applications. *Science* 2013, 339:535-539.

Donaldson, K., Poland, C.A., Schins, R.P. Possible genotoxic mechanisms of nanoparticles: criteria for improved test strategies. *Nanotoxicology* 2010, 4:414-420.

Dopp, E., Schuler, M., Schiffmann, D., Eastmond, D.A. Induction of micronuclei, hyperdiploidy and chromosomal breakage affecting the centric/pericentric regions of chromosomes 1 and 9 in human amniotic fluid cells after treatment with asbestos and ceramic fibers. *Mutat. Res.* 1997, 377:77-87.

Elder, A. Nanotoxicology: How do nanotubes suppress T cells? *Nature Nanotechnol.* 2009, 4:409-410.

Gross, O., Poeck, H., Bscheider, M., Dostert, C., Hannesschlager, N., Endres, S., Hartmann, G., Tardivel, A., Schweighoffer, E., Tybulewicz, V. *et al*. Syk kinase signalling couples to the Nlrp3 inflammasome for anti-fungal host defense. *Nature* 2009, 459:433-436.

Kahlenberg, J. M.; Dubyak, G. R., Mechanisms of caspase-1 activation by P2X7 receptor-mediated K+ release. *Am. J. Physiol. Cell Physiol.* 2004, 286:C1100-1108.

Kim, J.S., Lee, K., Lee, Y.H., Cho, H.S., Kim, K.H., Choi, K.H., Lee, S.H., Song, K.S., Kang, C.S., Yu, I.J. Aspect ratio has no effect on genotoxicity of multi-wall carbon nanotubes. *Arch. Toxicol.* 2011, 5:775-786.

Kisin, E.R., Murray, A.R., Sargent, L., Lowry, D., Chirila, M., Siegrist, K.J., Schwegler-Berry, D., Leonard, S., Castranova, V., Fadeel, B., Kagan, V.E., Shvedova, A.A. Genotoxicity of carbon nanofibers: are they potentially more or less dangerous than carbon nanotubes or asbestos? *Toxicol. Appl. Pharmacol.* 2011, 252:1-10.

Kuhlbusch, T.A.J., Fissan, H., Asbach, C. Nanotechnologies and environmental risks: measurement technologies and strategies. In: Linkov, I., Steevens, J., (eds), *Nanomaterials: Risks and Benefits*. Dordrecht: Springer; 2009, p. 233–243.

Martinon, F., Burns, K., Tschopp, J. The inflammasome: a molecular platform triggering activation of inflammatory caspases and processing of proIL-beta. *Mol. Cell* 2002, 10:417-426.

Maynard, A.D., Aitken, R.J. Assessing exposure to airborne nanomaterials: current abilities and future requirements. *Nanotoxicology* 2007, 1:26–41.

Muller, J., Decordier, I., Hoet, P.H., Lombaert, N., Thomassen, L., Huaux, F., Lison, D., Kirsch-Volders, M. Clastogenic and aneugenic effects of multi-wall carbon nanotubes in epithelial cells. *Carcinogenesis* 2008, 29:427-433.

Nasibulin, A.G., Pikhitsa, P.V., Jiang, H., Brown, D.P., Krasheninnikov, A.V., Anisimov, A.S., Queipo, P., Moisala, A., Gonzalez, D., Lientschnig, G., Hassanien, A., Shandakov, S.D., Lolli, G., Resasco, D.E., Choi, M., Tománek. D., Kauppinen, E,I. A novel hybrid carbon material. *Nature Nanotechnol.* 2007, 2:156-161.

Nygren, J., S. Suhonen, S., Norppa, H., Linnainmaa, K. DNA damage in bronchial epithelial and mesothelial cells with and without associated crocidolite asbestos fibers. *Environ. Molec. Mutag.* 2004, 44:477-482.

Palomäki, J., Välimäki, E., Sund, J., Vippola, M., Clausen, P.A., Jensen, K.A., Savolainen K., Matikainen, S., Alenius, H. Long, needle-like carbon nanotubes and asbestos activate the NLRP3 inflammasome through a similar mechanism. *ACS Nano* 2011, 5:6861-6870.

Pelegrin, P, Surprenant, A. Pannexin-1 mediates large pore formation and inter-leukin-1beta release by the ATP-gated P2X7 receptor. *Embo J.* 2006, 25:5071-5082.

Petrilli, V., Papin, S., Dostert, C., Mayor, A., Martinon, F., Tschopp, J. Activation of the NALP3 inflammasome is triggered by low intracellular potassium concentration. *Cell Death Differ.* 2007, 14:1583-1589.

Poland, C. A., Duffin, R., Kinloch, I., Maynard, A., Wallace, W. A., Seaton, A., Stone, V., Brown, S., Macnee, W., Donaldson, K. Carbon nanotubes introduced into the abdominal cavity of mice show asbestos-like pathogenicity in a pilot study. *Nature Nanotechnol.* 2008, 3:423-428.

Reddel, R.R., Ke, Y., Gerwin, B.I., McMenamin, M.G., Lechner, J.F., Su, R.T., Brash, D.E., Park, J.B., Rhim, J.S., Harris, C.C. Transformation of human bronchial epithelial cells by infection with SV40 or adenovirus-12 SV40 hybrid virus, or transfection via strontium phosphate coprecipitation with a plasmid containing SV40 early region genes. *Cancer Res.* 1988, 48:1904-1909.

Riteau, N., Gasse, P., Fauconnier, L., Gombault, A., Couegnat, M., Fick, L., Kanellopoulos, J., Quesniaux, V. F., Marchand-Adam, S., Crestani, B. *et al*. Extracellular ATP is a danger signal activating P2X7 receptor in lung inflammation and fibrosis. *Am. J. Respir. Crit. Care Med.* 2010, 182:774-783.

Roco, M.C., Mirkin, C.A., Hersam, M.C (eds). *WTEC Panel Report on Nanotechnology Research Directions for Societal Needs in 2020. Retrospective and Outlook.* World Technology Evaluation Center, Science Policy Reports. September 30, 2010. Springer, 2010.

Romagna, F. Series: 'current issues in mutagenesis and carcinogenesis'.12. Improved method of preparing bone marrow micronucleus assay slides. *Mutat. Res.* 1988, 206: 307-309.

Ryman-Rasmussen, J.P., Cesta, M.F., Brody, A.R., Shipley-Phillips, J.K., Everitt, J.I., Tewksbury, E.W., Moss, O.R., Wong, B.A., Dodd, D.E., Andersen, M.E., Bonner, J.C. Inhaled carbon nanotubes reach the subpleural tissue in mice. *Nature Nanotechnol*. 2009, 4:747-751.

Sakamoto, Y., Nakae, D., Fukumori, N., Tayama, K., Maekawa, A., Imai, K., Hirose, A., Nishimura, T., Ohashi, N., Ogata, A. Induction of mesothelioma by a single intrascrotal administration of multi-wall carbon nanotube in intact male Fischer 344 rats. *J. Toxicol. Sci.* 2009, 34:65–76.

Sargent, L.M., Reynolds S.H., Castranova, V. Potential pulmonary effects of engineered carbon nanotubes: in vitro genotoxic effects. *Nanotoxicology* 2010, 4:396-408.

Sargent, L.M., Hubbs, A.F., Young, S.H., Kashon, M.L., Dinu, C.Z., Salisbury, J.L., Benkovic, S.A., Lowry, D.T., Murray, A.R., Kisin, E.R., Siegrist, K.J., Battelli, L., Mastovich, J., Sturgeon, J.L., Bunker, K.L., Shvedova, A.A. and Reynolds, S.H. Single-walled carbon nanotube-induced mitotic disruption. *Mutat. Res.* 2012, 745:28-37.

Savolainen, K., Pylkkänen, L., Norppa, H., Falck, G., Lindberg, H., Tuomi, T., Vippola, M., Alenius, H., Hämeri, K., Koivisto, J., Brouwer, J., Mark, D., Bard, D., Berges, M., Jankowska, E., Posniak, M., Farmer, P., Singh, R., Krombach, F., Bihari, P., Kasper, G., Seipenbusch, M. Nanotechnologies, engineered nanomaterials and occupational health. *Safety Sci.* 2010, 48:957-963.

Schins, R.P., Knaapen, A.M. Genotoxicity of poorly soluble particles. *Inhal. Toxicol.* 2007, 19 Suppl 1:189-198.

Sund J, Palomäki J, Ilves M, Rydman E, Savinko T, Koivisto J, Vippola M, Greco D, Wolff H, Pylkkänen L, Savolainen K, Puustinen A, Alenius H. Hiilinanoputkien aiheuttamien terveysvaikutusten karakterisointi systeemitoksikologian avulla. Loppuraportti Työsuojelurahaston hankkeesta Nro 110168. Työterveyslaitos 2013. Tietoa Työstä.

Surrallés, J., Xamena, N., Creus, A., Catalán, J., Norppa, H., Marcos, R. Induction of micronuclei by five pyrethroid insecticides in whole-blood and isolated human lymphocyte cultures. *Mutat. Res.* 1995, 341:169–184.

Takagi, A., Hirose, A., Nishimura, T., Fukumori, N., Ogata, A., Ohashi, N., Kitajima, S., Kanno, J. Induction of mesothelioma in p53+/- mouse by intraperitoneal application of multi-wall carbon nanotube. *J. Toxicol. Sci.* 2008, 33:105-116.

Takagi, A., Hirose, A., Futakuchi, M., Tsuda, H., Kanno J. Dose-dependent mesothelioma induction by intraperitoneal administration of multi-wall carbon nanotubes in p53 heterozygous mice. *Cancer Sci.* 2012, 103:1001-1004.

Waters, M.D., Jackson, M., Lea, I. Characterizing and predicting carcinogenicity and mode of action using conventional and toxicogenomics methods. *Mutat. Res.* 2010, 705:184-200.

Woodrow Wilson International Center for Scholars (2011) *Project on Emerging Nanotechnologies. Consumer Products. An inventory of nanotechnology-based consumer products currently on the market.*
www.nanotechproject.org/inventories/consumer.

Yegles, M., Saint-Etienne, L., Renier, A., Janson, X., Jaurand, M.C. Induction of metaphase and anaphase/telophase abnormalities by asbestos fibers in rat pleural mesothelial cells in vitro. *Am. J. Respir. Cell Mol. Biol.* 1993, 9:186-191.

The development, production and technological applications of carbon nanotube are rapidly growing, due to the unique characteristics of these fibers. Consequently, an increase is also expected in human exposure to such materials. However, little is still known about the safety of the multiple sorts of carbon nanotubes.

Recent studies have suggested that some types of multi-walled carbon nanotubes (MWCNTs) have similar effects as asbestos. This report shows that rigid, long and needle-like MWCNTs induce inflammation and DNA damage in the lungs and in cultured cells, while flexible, long and tangled MWCNTs do not. It appears that the rigidity of MWCNTs is a key feature in triggering a specific inflammatory reaction and in causing cellular alterations involved in cancer formation.

These results provide new information on the adverse effects of MWCNTs and are useful in assessing which forms of MWCNTs require regulatory attention and special safety measures in occupational settings.

FINNISH INSTITUTE OF OCCUPATIONAL HEALTH

Topeliuksenkatu 41 a A, 00250 Helsinki
www.ttl.fi

ISBN 978-952-261-319-6 (paperback)
ISBN 978-952-261-320-2 (PDF)

Finnish Institute of Occupational Health

Työsuojelurahasto
Arbetarskyddsfonden
The Finnish Work Environment Fund